Technical and economic performance of the dithionite-assisted organosolv fractionation of lignocellulosic biomass

Filippo Brienza,[a, b] Korneel Van Aelst,[c] François Devred,[b] Delphine Magnin,[d] Maxim Tschulkow,[e] Philippe Nimmegeers,[e, f] Steven Van Passel,[e, g] Bert F. Sels,[b] Patrick Gerin,[a] Damien P. Debecker[b] and Iwona Cybulska*[a]*

[a] Earth and Life Institute (ELI), UCLouvain, Croix du Sud 2, 1348 Louvain-La-Neuve, Belgium.

[b] Institute of Condensed Matter and Nanoscience (IMCN), UCLouvain, Place Louis Pasteur 1, 1348 Louvain-La-Neuve, Belgium.

[c] Centre for Sustainable Catalysis and Engineering, KU Leuven, Celestijnenlaan 200F, 3001 Leuven, Belgium.

[d] Bio- and Soft Matter Division, Institute of Condensed and Nanosciences, UCLouvain, Croix du Sud 1, 1348 Louvain-la-Neuve, Belgium.

[e] Department of Engineering Management, University of Antwerp, Prinsstraat 13, 2000, Antwerp, Belgium.

[f] Intelligence in Processes, Advanced Catalysts and Solvents (iPRACS), Faculty of Applied Engineering, University of Antwerp, Groenenborgerlaan 171, 2020 Antwerp, Belgium.

[g] Nanolab Centre of Excellence, Prinsstraat 13, 2000, Antwerp, Belgium.

Abstract

The development of biomass pretreatment approaches that, next to (hemi)cellulose valorization, aim at the conversion of lignin to chemicals is essential for the long-term success of a biorefinery. Herein, we discuss a dithionite-assisted organosolv fractionation (DAOF) of lignocellulose in *n*-butanol and water to produce cellulosic pulp and mono-/oligo-aromatics. The present study frames the technicalities of this biorefinery process and relates them to the features of the obtained product streams. Via the extensive characterization of the solid pulp (by acid hydrolysis-HPLC, ATR-FTIR, XRD, SEM and enzymatic hydrolysis-HPLC), of lignin derivatives (by GPC, GC-MS/FID, ^{1}H-^{13}C HSQC NMR, and ICP-AES) and of carbohydrate derivatives (by HPLC) we comprehensively identify and quantify the different products of interest. These results were used for inspecting the economic feasibility of DAOF. The adoption of a dithionite loading of 16.7% $w/w_{biomass}$ and of an equivolumetric mixture of *n*-butanol and water, which led to a high yield of monophenolics (~20%, based on acid insoluble lignin, for the treatment of birch sawdust), was identified as the most profitable process configuration. Furthermore, the treatment of various lignocellulosic feedstocks was explored, which showed that DAOF is particularly effective for processing hardwood and herbaceous biomass. Overall, this study provides a comprehensive view of the development of an effective dithionite-assisted organosolv fractionation method for the sustainable upgrading of lignocellulosic biomass.

Keywords

Lignocellulose, Biorefinery, Organosolv, Dithionite, Lignin depolymerization

Graphical abstract

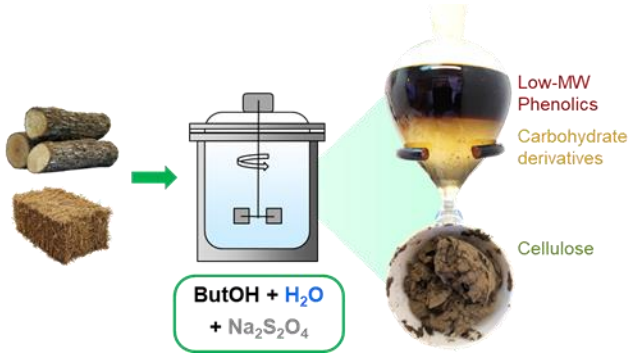

Sodium dithionite is used as an additive within organosolv fractionation to enhance the conversion of lignin toward valuable low-molecular weight phenolics and high-quality pulp.

INTRODUCTION

The use of lignocellulose for the sustainable production of energy, chemicals or materials was recognized as a promising alternative to fossil resources.[1–5] Lignocellulosic biomass is the most abundant source of renewable biomass on Earth and includes byproducts from forestry and wood processing (*e.g.* wood chips, sawdust, bark) as well as agricultural residues (*e.g.* wheat straw, corn stover) and so-called energy crops (*e.g.* miscanthus, switch grass).[6,7] As a composite biopolymer, lignocellulose is constituted of three main components: cellulose, hemicellulose and lignin, which are linked together to form a deeply intertwined structure. The high heterogeneity of this substrate, and the related recalcitrance toward bioprocessing,[8] imposed the adoption of an initial pretreatment in lignocellulose biorefineries, with the goal of reducing the complexity of the initial feedstock by disassembling lignocellulose structure,[8,9] before further conversion of the intermediates toward valuable end products (*e.g.* paper, bioethanol,[10] levulinic acid,[11] 5-HMF,[12] furfural,[12] phenol,[13,14] bionaphta[15], etc.). While several methods were developed for the pretreatment of lignocellulosic biomass, including physical methods (*e.g.* milling,[16,17] ultrasonication[18]), chemical methods (*e.g.* alkaline,[19,20] acid,[21,22] organosolv,[23,24], ionic liquids[25]) or mechanical-physicochemical methods (*e.g.* steam explosion,[26] ammonia fiber explosion[27]), the vast majority of them focused on the valorization of the carbohydrate fraction of biomass. From this point of view, the need for efficient strategies to convert lignin into value-added still constitutes a paramount challenge for biorefineries.[2,4,28–32]

Throughout the last few decades, a broad variety of processes were studied for the valorization of the technical lignins obtained upon biomass fractionation, such as pyrolysis or gasification,[32–35] reductive or oxidative depolymerization methods[28–33] and base- or acid-catalyzed methods.[28–32] However, due to the substantially degraded structure of technical lignins, their upgrading was

found to be challenging and high severity, energy-intensive methods often had to be employed, leading to mediocre yields and causing extensive defunctionalization of the produced lignin derivatives.[30–32]

Recently, a novel biorefining concept, targeting lignin depolymerization in the frame of biomass fractionation, received increasingly higher attention in the scientific community. This so-called "lignin-first" approach offers the opportunity to achieve a higher degree of valorization of lignocellulose components, with excellent preservation of their chemical functionalities.[28–31,36–39] Among the different methodologies that were proposed for lignin-first pretreatment, reductive catalytic fractionation (RCF) is particularly promising, as it allows to simultaneously isolate lignin from a carbohydrate pulp with high yields of delignification (up to about 90%, based on the initial lignin content in biomass) and to convert it toward valuable monophenolics with near-theoretical yields (up to 50-60%, based on the initial lignin content in biomass).[40,41] In spite of these inherent advantages, the use of precious metal catalyst and high pressures of hydrogen gas employed within RCF represent important limitations, imposing higher processing costs, as well as strict safety and equipment requirements.[41,42] The mechanism underlying RCF was elucidated in a study by Van den Bosch et al., who showed that lignin is extracted from biomass by solvolysis and labile ether bonds in lignin structures (predominantly β-O-4 linkages[3]) undergo reductive cleavage with the formation of reactive lignin units. The latter are ultimately stabilized against recondensation by catalytic hydrogenation of their unsaturated alkyl side chains.[43] A reductive cleavage of β-O-4 bonds was demonstrated to occur as well in a study conducted by Klinger et al. on the use of nucleophilic thiols for the depolymerization of pre-extracted, oxidized lignin, in which the authors reported a considerable production of monophenolics.[44,45] This process was explored further by

Fang et al. who developed an elegant thiol-assisted electrolytic approach for reductive lignin depolymerization.[46]

Inspired by these works, we recently reported the proof of concept for enhancing reductive depolymerization of lignin through the use of sodium dithionite ($Na_2S_2O_4$), an inexpensive and widely available sulfur-based reducing agent, as an alternative to precious metals and hydrogen gas, or nucleophilic thiols.[47,48] Such dithionite-assisted organosolv fractionation (DAOF) was shown to achieve superior conversion of lignin toward valuable monophenolics compared to a standard organosolv process, while concomitantly yielding a highly digestible cellulosic pulp. Moreover, the adoption of a *n*-butanol – water solvent combination conveniently facilitates product separation. Importantly, we demonstrated that the use of sodium dithionite triggers the reductive cleavage of β-O-4 bonds in lignin and the hydrogenation of unsaturated alkyl side chains in the generated phenolic units.[47]

Herein, we explore the techno-economic feasibility of DAOF by investigating the influence of process conditions on the features of the isolated product streams. The impact on the properties of the produced pulp, on lignin extraction and depolymerization, and on the yield of carbohydrate derivatives are analyzed in depth, with the goal of identifying the configuration which maximizes the process profitability, highlighting the current limitations and the potential future improvements of this technology. Finally, we explore the robustness of DAOF with respect to the treatment of biomass from different sources, including hardwood, softwood, and herbaceous feedstocks. We argue that DAOF represents an attractive strategy to implement lignin valorization within pulping, for a sustainable production of low-molecular weight phenolics.

EXPERIMENTAL SECTION

A full list of the materials used in this work and detailed descriptions of the experimental procedures and of the calculations performed are available in the ESI. Here, a condensed description of the main experimental process is provided.

Fractionation experiments

DAOF experiments were carried out in duplicates in a 300 mL Parr batch reactor (Figure S1, Parr Instrument Company, Moline, IL, U.S.): a chosen amount of biomass (3 – 12 g) was introduced in the reactor, together with 120 mL of a *n*-butanol – water mixture (*n*-butanol content: 0 – 100% v/v) and sodium dithionite (loading: 0% – 33% $w/w_{biomass}$). The air in the reactor was displaced by purging with N_2, then the reactor was pressurized with N_2 (1 or 30 bar). The impeller speed was set to 750 rpm and the temperature was increased at a rate of about 10 °C min^{-1}, up to a setpoint comprised between 150 °C and 250 °C. Once the setpoint was reached, the mixture was left to react for a duration of 0 to 6 hours.

Products separation and analysis

After each experiment, the reactor was cooled down to ambient temperature by letting water flow through the cooling coil, depressurized, and its content was collected. A solid and a liquid fraction were separated by centrifugation. The solid fraction was washed first with pure *n*-butanol (15 mL $g_{initial\ biomass}^{-1}$) and then with pure water (15 mL $g_{initial\ biomass}^{-1}$) to remove apolar and polar components weakly adsorbed to the pulp, then it was dried at 60 °C to a constant weight. Subsequently, the washing solvents were combined with the liquid fraction, and the mixture was filtered to eliminate residual solid particles. The filtrate was transferred to a separating funnel, where it separated into an organic and an aqueous liquid phase (Figure S2a), which were then collected. The retentate was recovered and added to the solid fraction.

Dry matter, ash, and organic matter contents were determined for all the isolated fractions.

The solid fraction (Figure S2b) was characterized via a battery of techniques, including acid hydrolysis followed by high-performance liquid chromatography (HPLC) analysis, attenuated total reflection-Fourier transform infrared spectroscopy (ATR-FTIR), X-ray powder diffraction (XRD) analysis, field emission gun scanning electron microscopy (FEG-SEM), and enzymatic saccharification followed by HPLC.

Portions of the organic liquid fraction were dried under nitrogen flow to remove the solvent, then underwent a three-fold liquid-liquid extraction with dichloromethane and water, to isolate lignin derivatives from more polar products. The dichloromethane fractions were mixed, and dried under vacuum to yield a viscous brown lignin oil (Figure S2c), which was subsequently analyzed via gel permeation chromatography (GPC), gas chromatography (GC) coupled with a mass spectrometry (MS) detector and a flame ionization detector (FID), and ^{1}H-^{13}C heteronuclear single quantum coherence (HSQC) nuclear magnetic resonance (NMR). Extraction of monophenolics from the organic fraction was performed by drying a portion of the organic fraction under nitrogen flow, then subjecting it to a six-fold liquid-liquid extraction with cyclohexane and water. Drying the mixed cyclohexane fractions to remove the solvent yielded a monomers-rich cyclohexane oil, which was characterized via GPC and GC-MS/FID. Additionally, the sulfur content of the organic fraction and the cyclohexane oil was assessed by inductively coupled plasma atomic emission spectroscopy (ICP-AES).

The pH of the aqueous liquid fraction was measured, and the non-condensed carbohydrate derivatives present in this fraction were quantified by HPLC.

RESULTS AND DISCUSSION

Dithionite-assisted organosolv fractionation: process outline

In order to determine the outcomes of different process configurations, unless otherwise specified, batch experiments were carried out in duplicates treating birch sawdust (*Betula pendula,* particle size ≤ 2 mm,[49] biomass composition reported in Table S1) in a mixture of *n*-butanol and water, at temperatures in a range between 150 and 250 °C, in the presence of different loadings of sodium dithionite. After the fractionation, a cellulose-rich solid pulp was recovered. Concomitantly, two liquid fractions were obtained: an organic fraction, comprising lignin derivatives and soluble humins, and an aqueous fraction, containing non-condensed carbohydrate derivatives (*e.g.* mono- and oligosaccharides, polyols and organic acids). An overview of the DAOF process is shown in Figure 1.

With the goal of improving the performance of DAOF of lignocellulosic biomass, we investigated the influence of different variables on the properties of the obtained fractions, including the operating temperature, the exogenous nitrogen pressure, the loading of sodium dithionite, the loading of biomass, the residence time, and the *n*-butanol/water ratio.

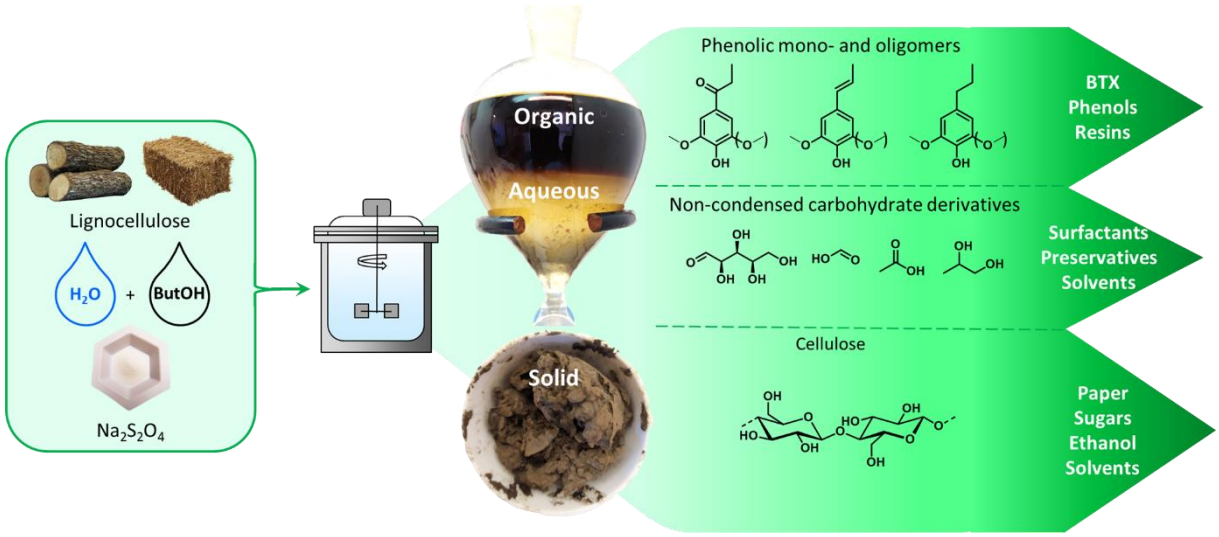

Figure 1 Outline of the dithionite-assisted organosolv fractionation of lignocellulosic biomass, with possible valorization routes for each product stream.

Lignocellulose disassembly and solubilization

The influence of process conditions on the solvolytic disassembly of lignocellulose was inspected by assessing the mass balance of organic matter (OM) with respect to the different fractions recovered (Figure 2 and Table S2). While the nitrogen pressure (Figure 2b and Table S2, entries 3, 6), the loading of dithionite (Figure 2c and Table S2, entries 3, 7 – 9) and that of biomass (Figure 2d and Table S2, entries 9 – 11) did not appear to substantially affect lignocellulose solubilization, the operating temperature, the residence time and the *n*-butanol/water ratio were recognized as key parameters in driving the solvolytic disassembly of biomass. Consistently with previous findings on hydrothermal and organosolv treatments,[50,51] increasing the temperature was found to promote the solubilization of lignocellulose components during DAOF, with a yield of pulp that diminished from 81% at 150 °C to 10% at 250 °C (Figure 2a and Table S2, entries 1 – 5). Analogously, extending the contact time from 0 hours (*i.e.* reaction halted as soon as the setpoint temperature was reached) to 6 hours resulted in a diminution of the pulp yield from 76% to 40%, accompanied by a gradual increase of the yield of soluble products (Figure 2e and Table

S2, entries 9, 12 – 14). Notably, the mass balance for OM was below 100% at temperatures greater than 150 °C and residence times longer than 0 hours, indicating an increasingly larger conversion of lignocellulose toward volatile components under more severe conditions (*e.g.* conversion of C5 and C6 polysaccharides toward formic acid and CO_2).[52–54]

The *n*-butanol/water ratio was also found to affect the pulp yield, which decreased from 65% in pure *n*-butanol to 44% upon addition of water, and was determined to be 53% in water alone, highlighting the synergetic effect of the *n*-butanol – water mixture with respect to lignocellulose disassembly (Figure 2f and Table S2, entries 9, 15 – 18). Correspondingly, the yield of liquid products was maximized when *n*-butanol and water were employed together. These observations can be explained by the dual nature of the solvent: on the one hand, *n*-butanol is more apolar than water and is less active toward solvolysis,[55] on the other hand, it possesses a higher ability to solubilize lignin and humins compared to water.[56,57] Interestingly, the mass balance was not affected by the *n*-butanol/water ratio, indicating that the formation of volatile products does not depend on this parameter.

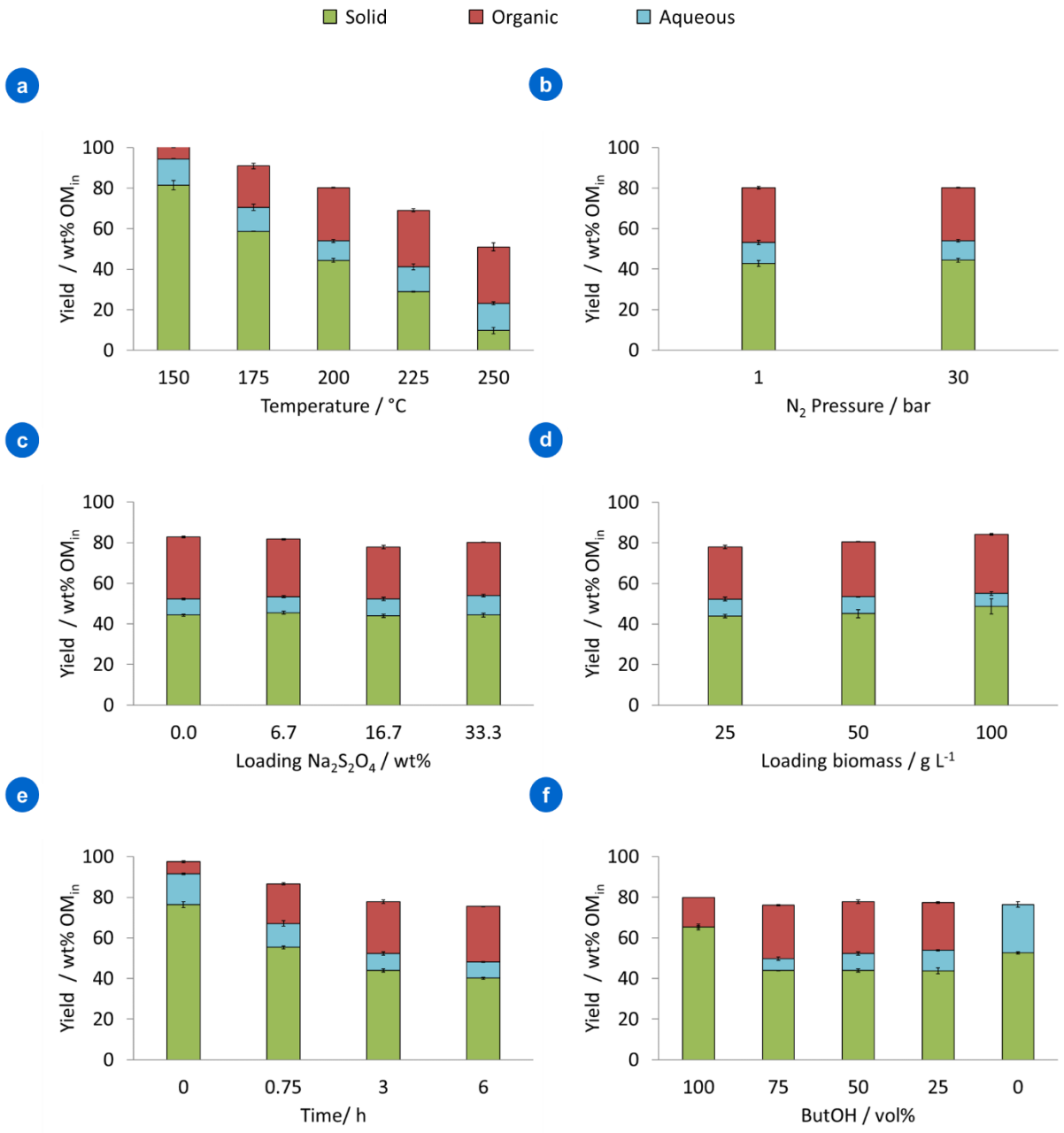

Figure 2 Influence of the operating temperature (a), the exogenous pressure (b) the loading of $Na_2S_2O_4$ (c), the loading of biomass (d), the residence time (e), and the *n*-butanol/water ratio (f) on the yield of OM recovered in the solid and liquid (organic and aqueous) fractions obtained after the dithionite-assisted organosolv fractionation of birch sawdust. Unless otherwise specified, fractionation experiments were performed treating 3 g of birch sawdust in 120 mL of a 50% v/v mixture of *n*-butanol and water, at 200 °C, under 30 bar of N_2 (introduced at ambient temperature), in the presence of $Na_2S_2O_4$ (33.3% w/$w_{biomass}$ for panels a and b ; 16.7% w/$w_{biomass}$ for panels d – f), for a duration of 3 hours.

The solid fraction: cellulosic pulp

The isolated solid fractions were subjected to acid hydrolysis, following a well-established procedure,[58] and their composition in terms of polysaccharides and lignin was determined (Table 1). Furthermore, the chemical and structural features of the different pulps, their cellulose crystallinity index (CI),[59] and their surface morphology were analyzed via ATR-FTIR spectroscopy (spectra reported in Figure S3, band assignments in Table S3), XRD analysis (Figure S4) and SEM (Figures S5-S8), respectively. Additionally, the effectiveness of the pretreatment with respect to enhancing the processability of the solid fractions was evaluated by assessing the enzymatic convertibility of the retained C5 and C6 polysaccharides (mainly xylan and glucan) toward monosaccharides (xylose and glucose) (Figure 3).[60]

Table 1 Biomass derivatives obtained for the DAOF of birch sawdust under varying process conditions.

Entry	Experimental conditions[a]						Solid Recovery[b] (wt%)			Organic Yield[c] (wt%)		Aqueous Yield[d] (wt%)
	T (°C)	P_{N_2} (bar)	$Na_2S_2O_4$ (wt%[e])	C_{biom} (g L^{-1})	t (h)	ButOH (vol%)	C5	C6	Lignin[f]	Oil	Mono	C5, C6 derivatives
1	150	30	33.3	25	3	50	83 ± 5	93 ± 2	128 ± 7	4 ± 1	1.2 ± 0.4	0.1 ± 0.0
2	175	30	33.3	25	3	50	43 ± 2	92 ± 3	77 ± 8	63 ± 1	5.9 ± 1.2	2.8 ± 0.2
3[f]	200	30	33.3	25	3	50	18 ± 3	92 ± 1	28 ± 3	93 ± 7	18.1 ± 1.7	7.5 ± 0.4
4	225	30	33.3	25	3	50	5 ± 2	68 ± 1	21 ± 6	121 ± 6	17.1 ± 2.5	2.8 ± 0.2
5	250	30	33.3	25	3	50	-	21 ± 7	11 ± 2	131 ± 7	11.2 ± 0.8	7.5 ± 0.4
6	200	1	33.3	25	3	50	15 ± 2	93 ± 2	27 ± 9	92 ± 2	17.7 ± 2.3	5.7 ± 0.3
7[g]	200	30	0.0	25	3	50	16 ± 1	93 ± 3	31 ± 9	95 ± 2	3.6 ± 0.6	3.4 ± 0.5
8	200	30	6.7	25	3	50	20 ± 2	91 ± 2	36 ± 2	90 ± 6	12.1 ± 1.3	2.6 ± 0.5
9	200	30	16.7	25	3	50	20 ± 2	92 ± 2	27 ± 3	93 ± 6	19.4 ± 1.8	4.0 ± 0.4
10	200	30	16.7	50	3	50	9 ±4	88 ± 5	54 ± 5	99 ± 1	18.2 ± 1.2	3.2 ± 0.5
11	200	30	16.7	100	3	50	11 ± 1	82 ± 4	66 ± 6	119 ± 2	16.7 ± 1.0	4.3 ± 0.4
12	200	30	16.7	25	0[h]	50	68 ± 5	93 ± 2	119 ± 5	10 ± 0	0.4 ± 0.2	0.5 ± 0.2
13	200	30	16.7	25	0.75	50	42 ± 3	95 ±2	54 ± 7	59 ± 5	9.9 ± 1.3	2.3 ± 0.5
14	200	30	16.7	25	6	50	9 ± 2	87 ± 5	26 ± 7	115 ± 5	20.6 ± 2.1	3.7 ± 0.8
15	200	30	16.7	25	3	100	69 ± 4	89 ± 3	69 ± 6	63 ± 5	6.6 ± 2.2	1.7 ± 0.4[i]
16	200	30	16.7	25	3	75	24 ± 2	89 ± 1	34 ± 3	96 ± 7	16.8 ± 1.6	3.5 ± 0.1
17	200	30	16.7	25	3	25	13 ± 1	94 ± 1	31 ± 6	84 ± 5	18.2 ± 1.8	2.6 ± 0.1
18	200	30	16.7	25	3	0	6 ± 0	80 ± 4	107 ± 4	44 ± 5[j]	4.1 ± 1.1[j]	2.5 ± 0.6

[a] Reactions were carried out in duplicates.

[b] Recovery of hemicellulose, cellulose and lignin in the solid fraction, expressed with respect to the weights of the different components in the dry initial biomass.

[c] Yield of lignin oil and phenolic monomers in the organic fraction, expressed with respect to the weight of acid-insoluble lignin contained in the initial biomass.

[d] Yield of non-condensed carbohydrate derivatives in the aqueous fraction, expressed with respect to the total weight of polysaccharides contained in the initial biomass.

[e] Expressed with respect to the weight of biomass introduced in the reactor.

[f] Acid-insoluble lignin.

[g] Experimental conditions investigated in our previous work.[47]

[h] Fractionation halted immediately after the setpoint temperature was reached.

[i] Determined in the organic fraction.

[j] Determined in the aqueous fraction.

Except for nitrogen pressure (Table 1, entries 3, 6 and Figure 3b) and for the loading of sodium dithionite (Table 1, entries 3, 7 – 9 and Figure 3c), all the considered process variables were found to exert an influence on the retention of polysaccharides, on delignification and on the pulp processability.

At a low treatment temperature of 150 °C most of the polysaccharides were found to be retained in the pulp, with recoveries of C5 and C6 polysaccharides of 83% and 93%, respectively (Table 1, entry 1). A lignin recovery of 128% was measured in the solid fraction, ascribable to the formation of pseudolignin (*e.g.* insoluble humins) and its deposition on cellulose fibers.[61–63] Processing at higher temperatures triggered the removal of hemicellulose and lignin (Table 1, entries 2 – 5), whereas the recovery of C6 polysaccharides remained rather constant up until 200 °C, above which cellulose hydrolysis increased markedly. These observations were confirmed by FTIR analyses of the solid fractions (Figure S3a), which showed that incrementing the treatment temperature above 150 °C resulted in the gradual disappearance of the bands at 1235 cm^{-1}, 1465 cm^{-1}, 1510 cm^{-1}, 1595 cm^{-1}, and 1740 cm^{-1}, assigned to lignin and hemicellulose, pointing out their removal from the pulps. On the other hand, for the solid fraction isolated after a treatment at 250 °C, a more marked band appeared at 1045 cm^{-1} in the FTIR spectrum (assigned to lignin), pinpointing the presence of a higher content of residual lignin relative to the amount of pulp isolated after severe treatment. Notably, the bands at 1160 cm^{-1} and 1098 cm^{-1} became more evident at higher temperatures, revealing a larger cellulose purity and a higher proportion of crystalline cellulose. Further XRD analyses of the pulps showed that their CIs increased with temperature from 42% at 150 °C to 56% at 225 °C (Figure 3a), owing to the removal of amorphous components (lignin and hemicellulose) from the solid fraction.[64,65] Remarkably, the pulp isolated at 150 °C possessed a CI lower than that of raw biomass. Such finding can be explained by the redeposition of

pseudolignin on cellulose fibers, which is known to negatively affect the CI.[64] SEM images of the raw biomass and of the solid fractions revealed that increasing the treatment temperature resulted in a gradually smoother surface and in the appearance of bundles of fibers that became thinner as the temperature was raised (Figure S5a – d). This indicates a partial disassembly of the fibrous structure, which is expected to enhance the enzymatic digestibility of the pulp.[66] In agreement with this, a larger convertibility of glucan and xylan was determined for the pulps obtained at higher temperatures (Figure 3a), reaching values greater than 90% above 175 °C, by virtue of an enhanced delignification and a higher accessibility of cellulose fibers.

The adoption of higher loadings of biomass resulted in a gradual diminution of the recovery of C5 and C6 polysaccharides, from 20% and 92% at 25 g L^{-1} down to 11% and 82%, respectively, at 100 g L^{-1} (Table 1, entries 9 – 11). We reason that the intermediates produced by carbohydrate degradation, including short organic acids,[52,53,67] may promote further (hemi)cellulose decomposition. At the same time, larger recoveries of lignin were measured, which may be due to a poorer lignin solvolysis or to pseudolignin formation. A larger presence of lignin at higher biomass loading was recognized also via FTIR analyses, with the bands at 1045 cm^{-1} and 1595 cm^{-1} that were more apparent at 100 g L^{-1} (Figure S3d). The band at 1098 cm^{-1} was also more evident at high biomass loading, indicating a larger content of crystalline cellulose in the pulp. XRD analyses revealed that no major change occurred in the CIs of the pulps obtained at different biomass loadings (Figure 3d). Such observation may be explained by the opposed effects that an increased content of amorphous (pseudo)lignin and a higher fraction of crystalline cellulose would exert on CI.[68] SEM images of the solid fractions showed that the adoption of high biomass loadings resulted in a rougher, more tightly packed fibrous structure (Figure S6a – c), possibly less susceptible toward enzymatic conversion.[50] Consistently, the digestibility of glucan was found to

decrease from 91% at 25 g L^{-1} to 77% at 100 g L^{-1} (Figure 3d), suggesting that the higher content of (pseudo)lignin and the more compact structure observed at higher loading limits cellulose accessibility for enzymatic attack.[50,63]

Increasing the residence time had a similar impact as raising the operating temperature (Table 1, entries 9, 12 – 14). While high recoveries of polysaccharides (68% for C5 and 93% for C6) and pseudolignin formation (lignin recovery of 119%) were observed at short residence times (*i.e.* "0 hours" condition), longer treatment durations resulted in the extensive removal of hemicellulose and lignin. These observations were substantiated by FTIR analyses of the solid fractions (Figure S3e), which showed that minor changes in the spectrum were apparent at very short reaction times (0 hours) compared to the raw biomass, whereas longer processing times resulted in the disappearance of the bands at 1235 cm^{-1}, 1465 cm^{-1}, 1510 cm^{-1}, and 1740 cm^{-1}, assigned to lignin and hemicellulose, and in the shrinkage of the band at 1595 cm^{-1}, assigned to lignin. The higher purity of cellulose at longer times was highlighted by the gradually more apparent band at 1160 cm^{-1}. In agreement with such findings, the CIs of the pulps increased with time from 44% at 0 hours up to 53% at 6 hours (Figure 3e). SEM analyses showed that the surface of the solid fraction isolated after 0 hours of treatment possessed a coarse morphology, much alike that of the raw biomass, and no fibers were apparent (Figure S7a, b). On the contrary, after 3 hours a more open fibrous structure could be observed (Figure S7c). Accordingly, the digestibility of glucan and xylan increased with the residence time, and values greater than 90% were measured for the pulps obtained after processing for 3 hours or longer (Figure 3e).

The effect of the *n*-butanol/water ratio on the properties of the isolated pulps confirmed the benefits deriving from the adoption of a mixture of *n*-butanol and water compared to the pure solvents (Table 1, entries 9, 15 – 18). When *n*-butanol was employed alone, only a marginal

removal of hemicellulose and lignin from the pulp was observed (31% for both components), whereas the introduction of water led to an improved solubilization of these components, and a sharp increase of cellulose purity in the pulp (up to 77%). The use of water alone led to extensive removal of C5 polysaccharides and a marginal decrease of the recovery of C6 polysaccharides, along with the formation of pseudolignin (lignin recovery of 107%), highlighting how a solvent that is too polar would not be convenient for DAOF, as it would lack the ability to solubilize lignin and humic products formed during the fractionation. FTIR analyses of the solid fractions showed that a treatment in pure *n*-butanol led to a decrease of the bands at 1235 cm^{-1} and 1510 cm^{-1} and to the disappearance of the band at 1740 cm^{-1}, assigned to hemicellulose and lignin (Figure S3f). Conversely, the introduction of water as a co-solvent resulted in the complete disappearance of the bands at 1235 cm^{-1}, and 1510 cm^{-1}, as well as a substantial reduction of the bands at 1465 cm^{-1} and 1595 cm^{-1}, pointing out a more extensive removal of hemicellulose and lignin. The use of water alone resulted in more apparent bands corresponding to lignin (1045 cm^{-1}, 1465 cm^{-1}, 1510 cm^{-1} and 1595 cm^{-1}), highlighting its worse solubilization or its increased redeposition on the pulp surface. In addition, the presence of a more evident band at 1098 cm^{-1} indicated a higher content of crystalline cellulose. Consistent with the improved removal of amorphous components, the CIs determined for the pulps obtained from processing with mixtures of *n*-butanol and water were found to be greater than those measured for the pure solvents (Figure 3f). Further inspection of the solid fractions via SEM revealed that a treatment in *n*-butanol caused a smoothening of the pulp surface and exposed tightly packed bundles of fibers, which were partially disassembled upon the addition of water to the mixture (Figure S8a – c). On the contrary, the use of water alone led to an extensive fragmentation of lignocellulose and a consequent redeposition of the debris on the fibers, which were completely covered (Figure S8d). In line with this, a higher digestibility of the retained

polysaccharides was measured when *n*-butanol and water were employed together, with the highest glucan conversion of 91% determined for an equivolumetric mixture of the two solvents (Figure 3f).

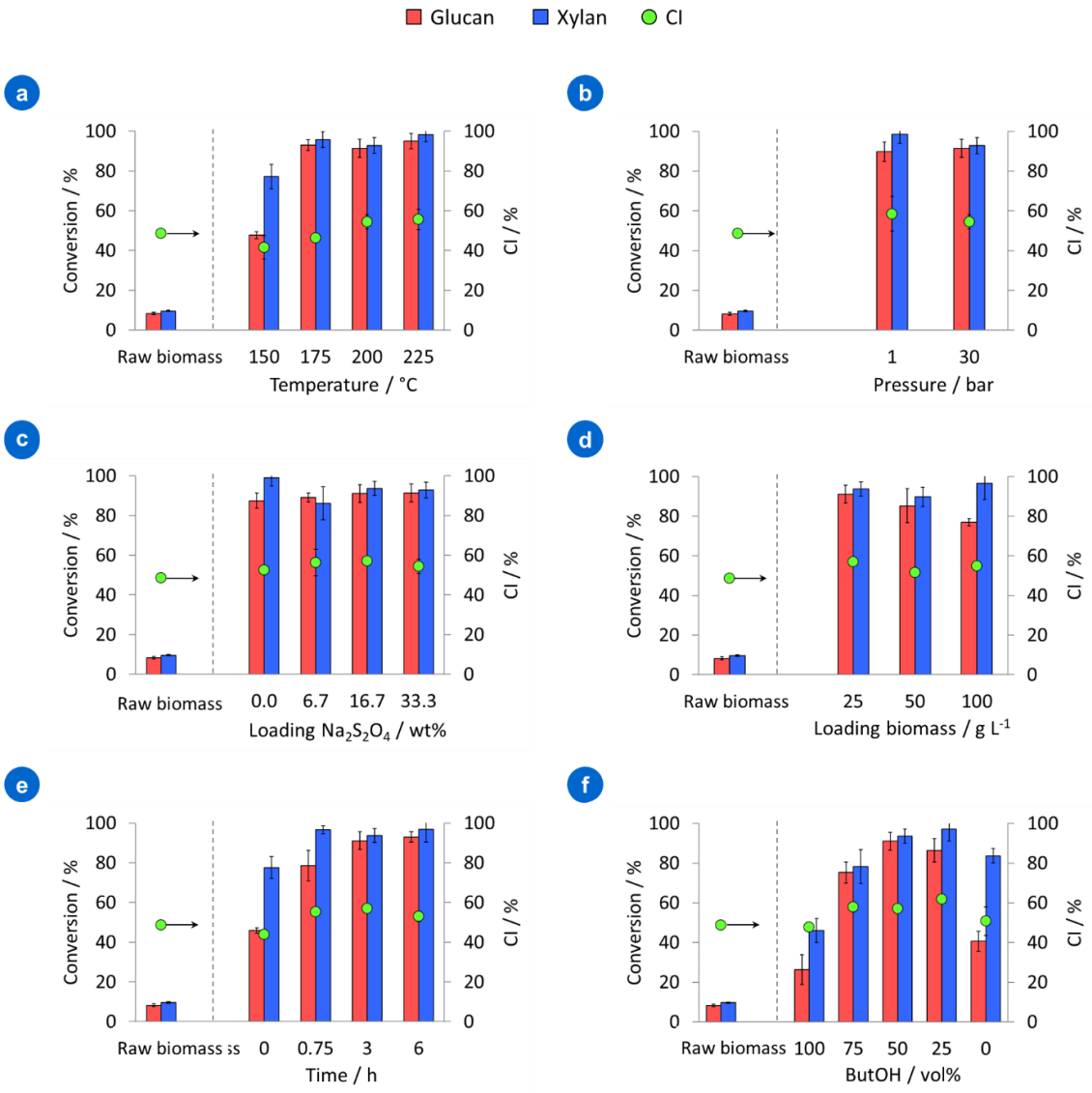

Figure 3 Influence of the operating temperature (a), the exogenous pressure (b) the loading of $Na_2S_2O_4$ (c), the loading of biomass (d), the residence time (e), and the *n*-butanol/water ratio (f) on the enzymatic digestibility and the cellulose crystallinity index of the solid fraction obtained after the dithionite-assisted organosolv fractionation of birch sawdust. Unless otherwise specified, fractionation experiments were performed treating 3 g of birch sawdust in 120 mL of a 50% v/v mixture of *n*-butanol and water, at 200 °C, under 30 bar of N_2 (introduced at ambient temperature),

in the presence of $Na_2S_2O_4$ (33.3% w/$w_{biomass}$ for panels a and b ; 16.7% w/$w_{biomass}$ for panels d – f), for a duration of 3 hours.

The organic fraction: lignin oil

The solubilized lignin was isolated from the organic liquid fractions via solvent evaporation followed by liquid – liquid extraction with dichloromethane and water, according to a procedure reported elsewhere.[43,69] Drying the dichloromethane extracts yielded viscous brown lignin oils, reported to comprise lignin derivatives and humic products.[47] The molecular weight distribution (MWD) of lignin oils and the phenolic monomers composition were determined via GPC and via gas GC-MS/FID, respectively.

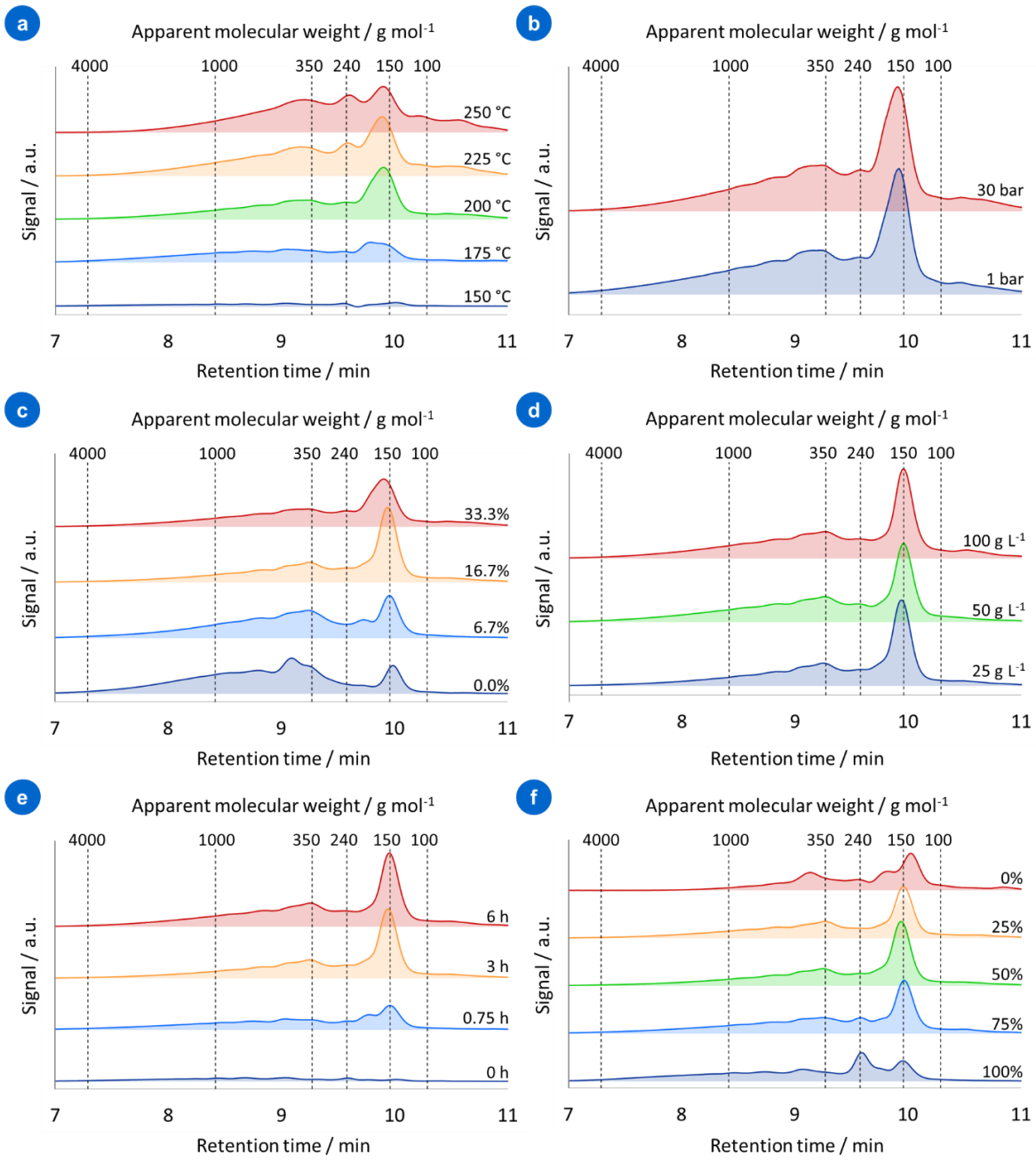

Figure 4 GPC chromatograms showing the influence of the operating temperature (a), the exogenous pressure (b) the loading of $Na_2S_2O_4$ (c), the loading of biomass (d), the residence time (e), and the *n*-butanol/water ratio (f) on the MWD of the lignin oil isolated from the organic fraction obtained after the dithionite-assisted organosolv fractionation of birch sawdust. Unless otherwise specified, fractionation experiments were performed treating 3 g of birch sawdust in 120 mL of a 50% v/v mixture of *n*-butanol and water, at 200 °C, under 30 bar of N_2 (introduced at ambient temperature), in the presence of $Na_2S_2O_4$ (33.3% $w/w_{biomass}$ for panels a and b ; 16.7% $w/w_{biomass}$ for panels d – f), for a duration of 3 hours. The area underneath each chromatogram was normalized with respect to the yield of lignin oil obtained for the corresponding experiment.

In line with previous reports on organosolv and RCF processes,[70,71] lignin solvolysis and the yield of lignin oil were found to increase substantially with temperature (Table 1, entries 1 – 5). A major increment of the yield of lignin oil from 4% to 63% was measured between 150 and 175 °C, pointing to a threshold temperature for achieving an effective solvolytic disassembly of lignin-carbohydrate linkages. Yields of oil greater than 100% were observed at high temperatures (>200 °C), highlighting the incorporation of humins in the oil, most probably generated upon the extensive decomposition of C5 and C6 polysaccharides achieved under these conditions.[63,72,73] GPC analyses of the lignin oils extracted at different temperatures are shown in Figure 4a. As the temperature was raised from 150 to 200 °C, a peak at about 150 g mol^{-1} appeared and became preponderant, indicating the enhanced formation of phenolic monomers. Further increase of the temperature resulted in a gradual disappearance of the monomers peak in favor of the formation of larger fragments, suggesting the occurrence of repolymerization reactions. Concomitantly, the formation of small fragments (M_W<100 g mol^{-1}) was observed, possibly corresponding to dealkylated monophenolics or carbohydrate derivatives (*e.g.* furans). Overall, the estimation of the average molecular weight (M_W) of lignin oils (Table S4, entries 1 – 5) clearly showed that M_W diminished as the operating temperature increased, with the highest drop of M_W, from about 1800 to 1000 g mol^{-1}, that was determined for the range 175 – 200 °C, corresponding to extensive formation of monophenolics. Consistently, GC-MS/FID analyses of the lignin oils revealed that the monomer yield increased with temperature, from 1.2% at 150 °C up to 18.1% at 200 °C, then diminished as the temperature was raised further (Figure 5a and Table S5). A broad variety of monomeric compounds was observed, including species with side chains containing carbonyl groups (**1 – 4**), species with 4-propenyl or 4-propyl side chains (**5** and **6**, respectively), and dealkylated species (**7**). Such a broad spectrum of products can be explained by the combination

of reductive and acid-catalyzed pathways for the cleavage of β-O-4 linkages in lignin.[47] Raising the operating temperature above 200 °C resulted in the gradual depletion of **1 – 4**, likely due to dealkylation and repolymerization reactions, as evidenced by the increased yield of **7** and by the presence of peaks at higher molecular weights observed in the GPC profiles. On the other hand, the consumption of **5** appeared to be accompanied by the formation of **6**, suggesting – as demonstrated with model compounds[47] – the ability of dithionite to promote the hydrogenation of double bonds in the side chains of lignin moieties at high temperature.

The nitrogen pressure was found to have virtually no influence on the yield and MWD of lignin oil (Table 1, entries 3, 6; Figure 4b and Table S4, entries 3, 6) as well as on the distribution of monophenolic products (Figure 5b and Table S6), confirming that effective valorization of lignin to monoaromatics could be achieved in the absence of external pressurization, thereby advantageously relaxing the equipment requirement to withstand moderate pressure (see below).

The loading of sodium dithionite did not appear to affect the yield of lignin oil, which remained around 90-95% (Table 1, entries 3, 7 – 9). On the contrary, dithionite loading was found to exert a major impact on lignin depolymerization (Figure 4c and Table S4, entries 3, 7 – 9). The GPC profiles in Figure 4c show that the introduction of dithionite within the fractionation process led to a considerable boost of the phenolic monomers fraction, accompanied by a gradual flattening of the tail extending to high molecular weights, which confirms the essential role of dithionite with respect to enhancing lignin depolymerization and partially preventing its recondensation. Importantly, the adoption of a dithionite loading of 16.7% $w/w_{biomass}$ led to a monomers peak in the chromatogram comparable to that observed for a loading of 33.3%, as well as to a similar M_W, suggesting that the amount of dithionite fed to the process could be advantageously reduced, compared to what we reported in our previous study on DAOF.[47] The effective production of

monophenolics was confirmed by GC analyses of the lignin oils, which showed that the highest yield of 19.4% was attained at a loading of 16.7% (Figure 5c, Table S7). Most strikingly, the loading of reducing agent was found to remarkably affect the monophenolics composition (Figure 5c, Table S7). In the absence of dithionite, a low yield of monomers of 3.6% was obtained, mainly comprising **1**, **2**, and **5**. The use of a dithionite loading of 6.7% resulted in a substantial increase in the formation of **5** (with a yield of 10.5%), highlighting an enhanced reductive cleavage of inter-unit linkages in lignin structures in the presence of the reducing agent.[47] Further increase of the dithionite loading to 16.7% boosted the yield of **5** up to 15.5%, and also led to a slightly larger formation of species with side chains containing carbonyl groups (**1** – **4**). Surprisingly, the use of a higher loading of 33.3% resulted in a diminution of the yield of **5** (down to 5.1%) and in larger yields of **1**, **2**, and **4**, possibly indicating a worse performance of dithionite with respect to the reductive cleavage of lignin in this scenario. A tentative explanation for such behavior could be found in the tendency of the reducing agent to undergo auto-catalytic decomposition in acidic aqueous media.[74–77]

The yield of lignin oil increased from 93% to 119% when the biomass loading was increased from 25 to 100 g L^{-1} (Table 1, entries 9 – 11), pointing to a larger incorporation of humins in the oil, in agreement with the lower recoveries of C5 and C6 polysaccharides discussed above. The MWD of the lignin oils showed a considerable formation of monophenols at all biomass loadings (Figure 4d and Table S4, entries 9 – 11), with a slightly more apparent tailing in the GPC profiles observed at higher loadings, suggesting incomplete lignin depolymerization or enhanced repolymerization. Further inspection by GC analysis revealed a slight decline of the overall yield of monomers with increasing biomass loading (Figure 5d and Table S8), and a rather uniform diminution of the yield of **1 – 5**, possibly due to their participation in recondensation reactions.

Concomitantly, **6** was formed, highlighting the partial hydrogenation of unsaturated alkyl side chains in lignin moieties, achieved as a result of the larger concentration of dithionite in the medium.

Longer residence times resulted in larger yields of lignin oil, corresponding to the progressive solubilization of lignin (Table 1, entries 9, 12 – 14). A yield of 115% was obtained after 6 hours, indicating the incorporation of humic products in the oil. The MWD of the oil was also affected by the processing time (Figure 4e and Table S4, entries 9, 12 – 14), with the appearance of a monomers peak in the GPC profile at 0.75 hours that increased at longer times. A tail extending to higher molecular weights was observed that gradually became more evident with time, suggesting partial repolymerization or the extraction of larger lignin fragments from the lignocellulose matrix.[78] GC analysis corroborated GPC results, showing that moderate production of monophenolics was achieved at 0.75 hours, with a yield of monomers of 9.9% and a high selectivity toward **5** and **3** (Figure 5e and Table S9). Longer residence times led to an increase of the yield of monomers up to 20.6% after 6 hours, with a boost of the selectivity toward **5** (up to about 80%) and a diminution of the selectivity toward **3**, possibly due to repolymerization reactions. The formation of monophenolics with shorter or missing alkyl side chains (**1**, **2**, **7**) was detected at longer times, indicating the occurrence of dealkylation reactions. The marginal production of **6** pinpoints the partial hydrogenation of lignin moieties under the action of dithionite.

Processing lignocellulosic biomass in pure *n*-butanol and pure water led to lignin oil yields of 63% and 44%, respectively (Table 1, entries 9, 15 – 18). On the other hand, the combined use of the two solvents resulted in substantially larger oil yields (up to 96%), clearly highlighting the superior performance of the mixture for the extraction of lignin. GPC analyses of the lignin oils showed that the adoption of *n*-butanol alone yielded a lignin oil with the highest M_W of ~1800 g

mol^{-1}, due to the poor disassembly of the extracted lignin and the high solubility of large lignin fragments in *n*-butanol. On the contrary, the use of water alone led to the lowest M_W of ~450 g mol^{-1} (Table S4 entries 9, 15 – 18). The latter observation is chiefly due to the low solubility of larger fragments in water, rather than to a more extensive depolymerization of lignin, as illustrated by the relatively flat GPC profile at high molecular weights, and by the small peak corresponding to lignin monomers (Figure 4f). Indeed, the best conditions for lignin depolymerization coincided with the use of a mixture of the two solvents, which led to a marked boost of the peak for monophenolics, up to a maximum achieved for the case of an equivolumetric mixture. Further inspection of the yield of lignin monomers via GC confirmed the conclusions made based on GPC (Figure 5f and Table S10). The yield of monophenolics was substantially increased by the combined use of *n*-butanol and water, up to a maximum of 19.4%, achieved for an equivolumetric mixture. A relevant finding is that a high yield of monophenolics of 18.2% could also be attained in the presence of a low fraction of *n*-butanol (25% v/v), suggesting that the amount of *n*-butanol co-solvent used for the fractionation could be conveniently diminished without substantially affecting the production of monoaromatics.

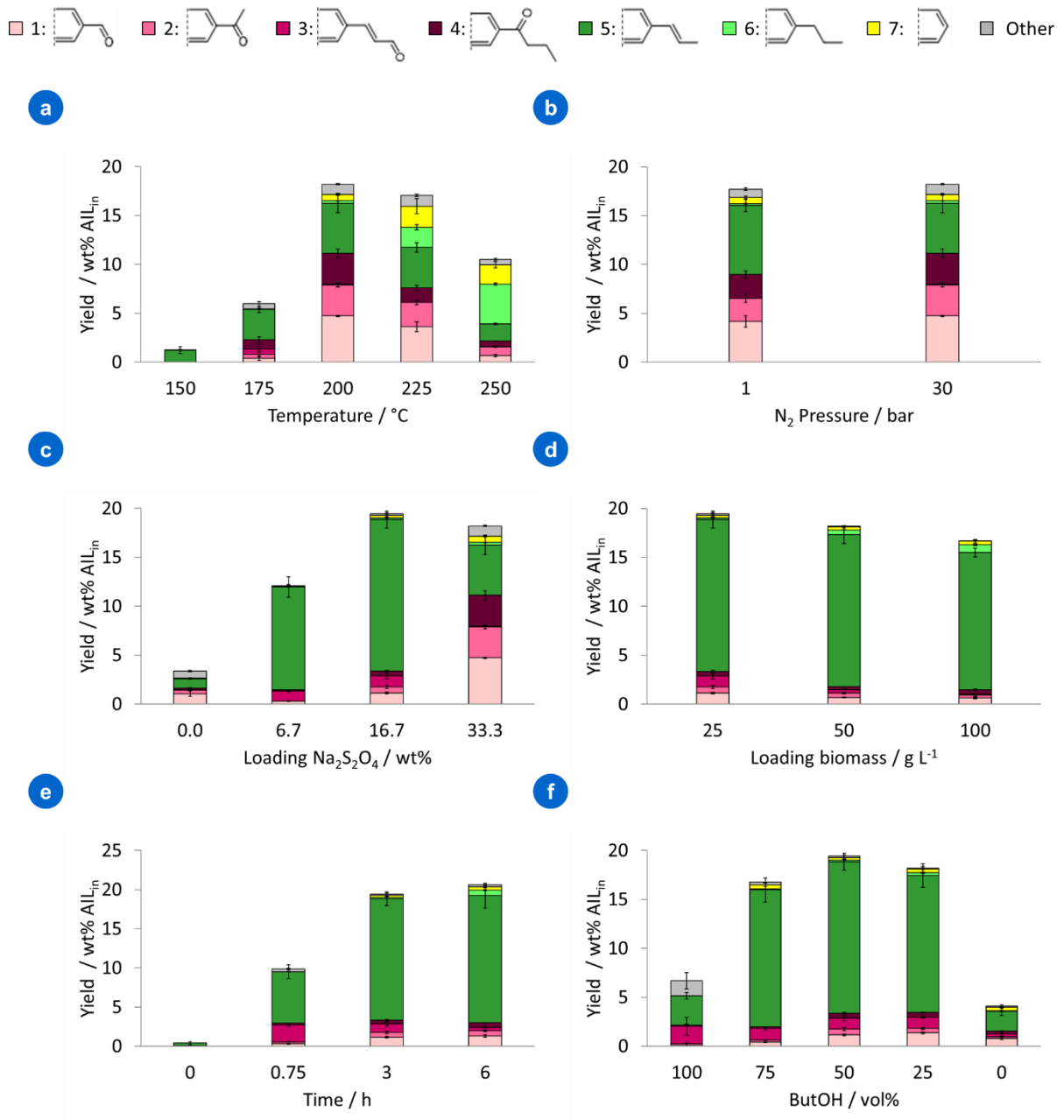

Figure 5 GC analyses showing the influence of the operating temperature (a), the exogenous N_2 pressure (b) the loading of $Na_2S_2O_4$ (c), the loading of biomass (d), the residence time (e), and the *n*-butanol/water ratio (f) on the yield of phenolic monomers in the lignin oil isolated from the organic fraction obtained after the dithionite-assisted organosolv fractionation of birch sawdust. Unless otherwise specified, fractionation experiments were performed treating 3 g of birch sawdust in 120 mL of a 50% v/v mixture of n-butanol and water, at 200 °C, under 30 bar of N_2 (introduced at ambient temperature), in the presence of $Na_2S_2O_4$ (33.3% w/$w_{biomass}$ for panels a and b ; 16.7% w/$w_{biomass}$ for panels d – f), for a duration of 3 hours. The monomer yield was calculated with respect to the acid insoluble lignin (AIL) content in the initial biomass.

With the goal of gaining further insight into the structural features of the aromatic species produced during DAOF, samples of lignin oil were subjected to ^{1}H-^{13}C HSQC NMR analysis. In particular, samples obtained in the presence of different loadings of dithionite were analyzed, to investigate the role of the reducing agent with respect to the formation of defined structural patterns (Table S11). In agreement with the previously discussed GC results, Figures S9 – S12 and the data reported in Table S12 clearly show that the use of a dithionite loading of 16.7% boosted the formation of species possessing 4-propenyl side chains compared to a treatment carried out in the absence of dithionite. At the same time, a slightly larger formation of 4- propenal end-units and other structural motifs containing carbonyl groups in their side chains (*e.g.* acetosyringone, acetoguaiacone, etc.) was observed. Further increase of the loading of reducing agent led to a sharp diminution of the signals corresponding to 4-propenyl and 4-propenal end-units and a remarkable increment of those corresponding to syringaldehyde, acetosyringone and acetoguaiacone structural motifs. These results confirm that the adoption of a dithionite loading of 16.7% efficiently provoked the reductive cleavage of β-O-4 linkages in lignin during DAOF. Interestingly, the formation of 4-propyl and 4-propanol end-units was determined in the presence of dithionite, pointing out its ability to reduce double bonds in the alkyl side chains of lignin moieties formed upon reductive cleavage of β-O-4 bonds.[47] Lignin inter-unit linkages were also found to be affected by the loading of the reducing agent. Notably, β-O-4 bonds were depleted more extensively at higher dithionite loadings, in line with the trend observed in a previous study with lignin model compounds.[47] Similarly, the signals corresponding to other native lignin linkages such as β-β resinol and β-5 phenylcoumaran were found to decrease at higher dithionite loadings, likely due to the cleavage of labile ether bonds in these structures.[29] In the absence of dithionite, only a low portion (~25%) of the ^{13}C–^{1}H HSQC spectrum could be assigned to known structural motifs (Table

S12). The unassigned portion of the spectrum may be associated with the formation of non-native C-C linkages between lignin units, resulting from repolymerization reactions.[79] Remarkably, in the presence of dithionite, the unassigned portion of the spectrum was lower compared to that determined in the absence of the reducing agent, suggesting that dithionite can partially prevent lignin recondensation, in line with the lower amount of high-M_W fragments and of the higher yields of monophenolics observed via GPC and GC analysis. Overall, ^{1}H-^{13}C HSQC NMR analysis showed that the dithionite loading has a marked impact on the end-units and inter-unit linkages in lignin derivatives (which will ultimately affect the physicochemical properties of the obtained lignin oil).

Phenolic monomers possessing unsaturated alkyl side chains were reported to form during biomass fractionation and to be particularly prone to undergo recondensation reactions.[29] In this respect, the formation of 4-propenyl-, 4-propenol- and 4-propenal-substituted monophenolics was observed during DAOF under mild conditions. At low temperature and short residence times these compounds were present in lignin oil (Table S5, Table S9). Similarly, they were observed for a treatment performed in pure *n*-butanol (Table S10). On the contrary, the adoption of moderate conditions resulted in the gradual disappearance of monomers with 4-propenol and 4-propenal side chains, and in an increased formation of species possessing 4-propenyl side chains. Larger fractions of high-M_W components were also determined (Figure 4a, e and f). Harsher treatment conditions resulted in the depletion of monomers possessing 4-propenyl side chains. Concomitantly, the formation of species with 4-propyl side chains and that of high-M_W components was observed (Figure 4a, e and f). Taken altogether, these findings suggest that monomers with 4-propenol and 4-propenal side chains are formed during DAOF, but are not stable and they either end up participating in repolymerization reactions, or undergo the loss of terminal

groups to yield 4-propenyl side chains. The latter may in turn undergo repolymerization or be reduced further by dithionite, as summarized in Scheme 1.

Scheme 1 Fate of phenolic monomers possessing unsaturated alkyl side chains during DAOF.

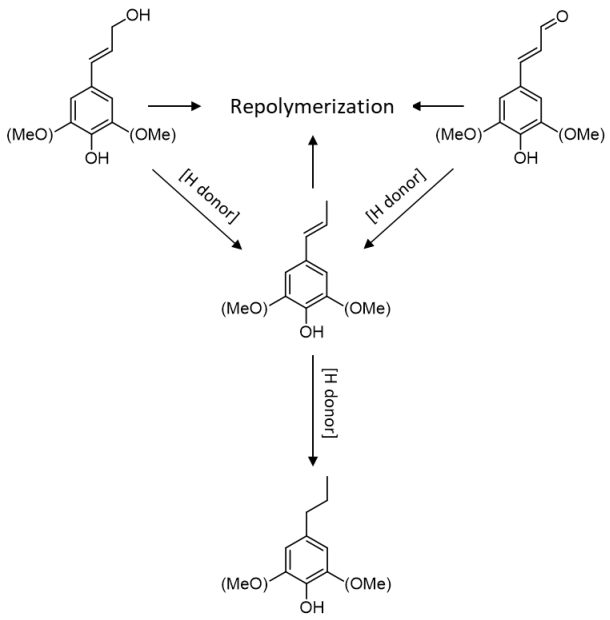

Effective isolation of phenolic monomers from the organic fraction represents an aspect of primary importance for their subsequent conversion toward valuable end products. Previous works on RCF showed that a liquid-liquid extraction of lignin oil with water and *n*-hexane could be used to isolate monophenolics, which tend to migrate toward the *n*-hexane phase, from more polar oligomers.[69,80] Cyclohexane was also reported to be a suitable solvent for the extraction of phenolic monomers after RCF.[81] Here, samples of the organic fractions obtained from DAOF were dried and subjected to six consecutive extractions with cyclohexane and water, to inspect the possibility of producing a relatively pure stream of monophenolics. Drying the combined cyclohexane fractions yielded an oil corresponding to 42% of the weight of acid insoluble lignin contained in the initial biomass. The analysis of the GPC profile observed for the cyclohexane oil showed the presence of a large peak corresponding to phenolic monomers, as well as a considerably reduced

tailing compared to the profile obtained for dichloromethane oil (Figure S13), demonstrating that efficient isolation of lignin monomers from heavier compounds could be achieved. GC analysis further confirmed this result and about 80% of the produced monophenolics were successfully recovered in the cyclohexane oil (Table S13).

A considerable formation of dithionite derivatives migrating to the organic fraction together with lignin components was reported in our previous work on DAOF.[47] With the goal of inspecting the extent of sulfur incorporation in the cyclohexane oil, it was subjected to ICP-AES analysis. While 48% of the sulfur initially introduced with the reducing agent was recovered in the organic fraction, only 9% of it was found in the cyclohexane oil, indicating that the extraction not only was effective for isolating monophenolics, but also afforded a stream of low-molecular weight lignin derivatives with a lower sulfur content.

The aqueous fraction: non-condensed carbohydrate derivatives

Even though the aqueous liquid fraction is ultimately considered as wastewater in the process, it was analyzed with the goal of gaining a more complete insight in fate of biomass and dithionite derivatives during DAOF. Thus, the aqueous liquid fractions obtained from DAOF were subjected to pH measurement and HPLC analysis to determine the influence of different process configurations on the acidity of the medium and on the production of xylose, 1,2 propanediol and formic acid, which were recognized as the major non-condensed carbohydrate derivatives formed during DAOF.[47] As a general trend, rather low yields of carbohydrate derivatives were measured for the different process configurations that were explored (Table 1). Consistently with this observation, the intermediates formed during (hemi)cellulose solvolysis were reported to be more prone to undergo degradation/recondensation compared to lignin derivatives.[82] Yet, all the studied

process variables (except nitrogen pressure – Figure S14b and Figure S15b) were found to affect the acidity of the medium and the formation of non-condensed carbohydrate derivatives.

A treatment temperature of 150 °C led to a low pH of 3.4 and to the formation of acetic acid, most probably resulting from deacetylation of hemicellulose.[83] The pH increased sharply at 175 °C, then remained around pH 6 at higher temperatures (Figure S14a). We surmise this behavior may be due to the partial decomposition of dithionite, as previously reported by other authors.[75] On the other hand, almost no production of carbohydrate derivatives was measured at 150 °C (Figure S15a). Such observation can be explained by the little solvolysis of (hemi)cellulose occurring at these conditions (see above). The yield of 1,2 propanediol and formic acid increased consistently up to 1.2% and 6.3%, respectively, at 200 °C, pointing to an enhancement of carbohydrate decomposition.[52,53] Further rise of the operating temperature caused a diminution of the yield of formic acid, possibly due to its conversion toward volatile products.[52]

Higher loadings of dithionite led to an increase of the pH despite the presence of larger concentrations of formic and acetic acid in the medium (Figure S14c), suggesting an increment of dithionite decomposition.[74–77] The gradual decline of the yield of xylose and the concomitant boost of the yield of formic acid at increasing dithionite loadings, indicate that dithionite promotes carbohydrate decomposition during DAOF, with a total yield of non-condensed carbohydrate derivatives that increased with the loading of the reducing agent from 3.4% in the absence of dithionite to 7.5% at a loading of 33% $w/w_{biomass}$ (Figure S15c). An analogous behavior was observed for experiments at different biomass loadings. The pH remained stable at 4.7 even though the concentrations of formic and acetic acid increased with the biomass loading (Figure S14d). In addition, Figure S15d shows a buildup of the yield of formic acid at the expense of xylose at higher biomass loadings (*i.e.* higher dithionite concentration in the medium). We surmise that, similarly

to the action of bisulfite ions during acid sulfite pulping,[22,84] dithionite could contribute to carbohydrate degradation by reacting with sugars to yield organic acids. Formic acid may be formed via further fragmentation reactions.[85]

Halting the fractionation immediately after reaching the setpoint temperature (*i.e.* "0 hours" experiment) resulted in the formation of acetic acid and in a low pH of the medium of 4.1 (Figure S14e). At longer residence times, the pH rose up to 4.7 in view of the action of dithionite.[75] Consistently with the high recoveries of C5 and C6 polysaccharides determined in the solid fraction, a minimal formation of carbohydrate derivatives was determined at a short residence time (Figure S15e). Conversely, longer durations resulted in the increase of the yields of xylose, 1,2 propanediol and formic acid, by virtue of a more extensive solvolysis of (hemi)cellulose.

The decrease of the *n*-butanol/water ratio led to a decline of the pH of the medium from 4.7 at 75% *n*-butanol v/v, to 3.9 in pure water, possibly due to a more effective deacetylation of hemicellulose (Figure S14f). The presence of *n*-butanol in the solvent mixture appeared to favor the production of formic acid, which reached a maximum of 2.8% for a mixture containing 75% *n*-butanol v/v. On the contrary, the use of greater amounts of water led to a decrease of the yield of formic acid, and a gradually larger yield of xylose (Figure S15f), pointing to the crucial role of solvent composition with respect to the fate of solubilized carbohydrates during DAOF.

Economic feasibility of DAOF

A techno-economic assessment (TEA) was conducted to study the economic feasibility of the DAOF process. From the process flow diagram (Figure 6) three product streams of interest were identified: a cellulosic pulp, a monophenolic-rich stream (cyclohexane oil), and an oligophenolic-rich stream (residue obtained after the extraction of monophenolics with cyclohexane). The

aqueous stream was considered as wastewater. The TEA presented by Tschulkow et al. for reductive catalytic fractionation (RCF) was used as a starting point for the present assessment.[86] As many similarities exist between the DAOF and RCF processes with respect to unit operations and plant sections needed, the CAPEX was assumed to be the same for RCF and DAOF (Table S14). This assumption makes the present TEA more conservative since DAOF does not rely on the use of heterogeneous catalysts or hydrogen gas, and lower temperatures and pressures are adopted, resulting in less stringent safety requirements and, overall, in a less costly reactor design. Moreover, it was assumed that the efficiency of the solvent recovery steps within DAOF was equal to that reported for RCF.[13,86]

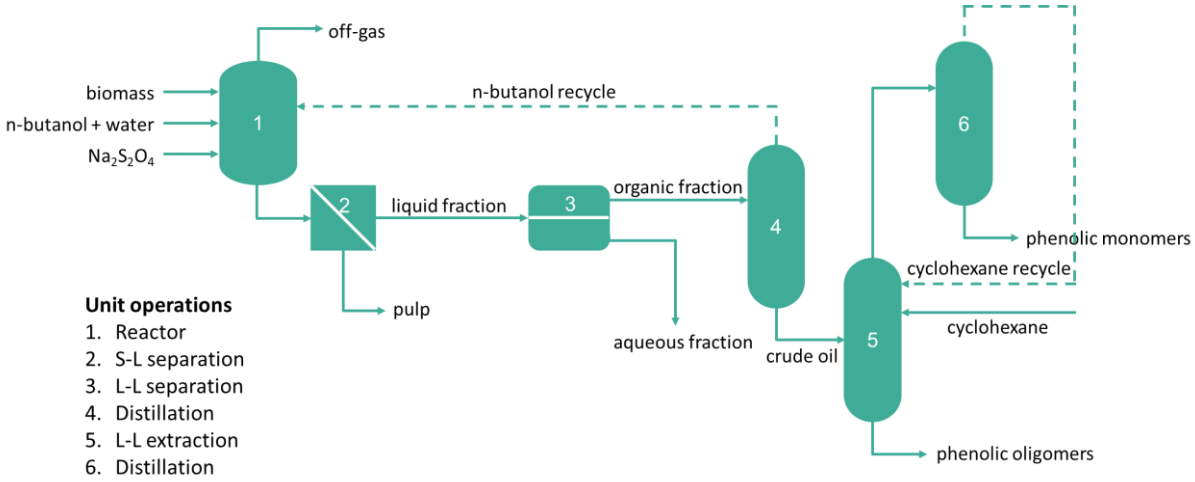

Figure 6 Flow diagram depicting the basic unit operations for the DAOF process. Streams for solvents recycle are indicated with dashed lines.

As the DAOF process is still at the proof-of-concept stage (technology readiness level (TRL) of 3-4), a higher discount rate of 17.5% was considered for DAOF, versus 15% for the more mature RCF (TRL 4-5). A project lifetime of 20 years was fixed, with an annual operating time of 8000 hours. Based on these hypotheses and assuming that the experimental data discussed in the previous sections were scalable, the net present value (NPV) for the DAOF configuration

corresponding to Table 1, entry 9, which led to the maximum yield of monophenolics, was calculated. Under the current assumptions (see operative expenditures (OPEX) and revenues in Table S15 and Table S16, respectively), such DAOF configuration appeared not to be economically feasible, leading to NPVs of -43, -81 and -104 M€ y^{-1} for annual dry birch wood intakes 20, 75 and 150 kt y^{-1}, respectively. From Table S15, sodium dithionite was found to contribute to a large fraction of the OPEX, suggesting lower amounts of dithionite could be more favorable.

Thus, the influence of the loading of dithionite on the NPV of DAOF was evaluated, according to the experimental configurations reported in Table 1, entries 3, 7 – 9. The yields of pulp, phenolic monomers and oligomers for these configurations are summarized in Table S17. In view of the extensive variability of the market price for monophenolics reported in the literature (2000 – 12000 € t^{-1}),[69,86,87] a conservative price range from 1500 to 6500 € t^{-1} was considered for this study. The outcomes of the analysis are reported in Table 2. Herein, four different regions can be distinguished: (i) for monomers selling prices lower than or equal to 3000 € t^{-1}, the DAOF process would not be economically feasible, (ii) for selling prices between 3500 € t^{-1} and 5500 € t^{-1} a *blank* organosolv process (performed in the absence of dithionite) would be the most convenient, (iii) for a price of 5500 € t^{-1} the process configuration with a dithionite loading of 6.7% $w/w_{biomass}$ would be the most favorable and (iv) for a price equal or greater than 6000 € t^{-1} the configuration with a dithionite loading of 16.7% would be the most promising.

Table 2 NPVs calculated for DAOF configurations using different dithionite loadings.

Monomers price (€ t^{-1})	NPV (M€ y^{-1})[a]			
	$Na_2S_2O_4$ loading (wt%)[b]			
	0.0	6.7	16.7	33.3
1500	-12.0	-63.2	-112.6	-199.4
2000	-8.5	-53.3	-96.8	-184.6
2500	-5.1	-43.4	-81.1	-169.9
3000	-1.7	-33.6	-65.3	-155.1
3500	1.7	-23.7	-49.5	-140.3
4000	5.1	-13.8	-33.7	-125.6
4500	8.5	-4.0	-17.9	-110.8
5000	11.9	5.9	-2.2	-96.1
5500	15.3	15.8	13.6	-81.3
6000	18.7	25.6	29.4	-66.6
6500	22.1	37.5	45.2	-51.8

[a] Calculated for a birch feedstock capacity level of 150 kt y^{-1}. (Orange fill: negative NPVs; Blue fill: positive NPVs).
[b] Expressed with respect to the weight of biomass.

Besides the cost of dithionite, that of *n*-butanol represented as well a considerable expenditure (Table S15), and the use of lower amounts of *n*-butanol could be more favorable. Therefore, a second sensitivity analysis was carried out to evaluate the effect of the *n*-butanol/water ratio on the NPV of DAOF, according to the experimental results reported in Table 1, entries 9, 15 – 18. The yields of pulp, phenolic monomers and oligomers for these configurations are summarized in Table S18. The outcomes of such analysis are illustrated in Table 3. As a result of the low amount of monophenolics produced in the presence of the pure solvents, neither the use of *n*-butanol or water alone led to economically feasible configurations. On the other hand, for monomers selling prices equal to or greater than 5500 € t^{-1}, the DAOF configurations with 25% and 50% *n*-butanol were found to be feasible, with the use of an equivolumetric mixture of *n*-butanol and water resulting in the largest NPVs.

Table 3 NPVs calculated for DAOF configurations using different *n*-butanol/water ratios.

Monomers price (€ t^{-1})	NPV (M€ y^{-1})[a]				
	n-butanol/water (%vol ButOH)				
	100	75	50	25	0
1500	-184.2	-130.4	-112.6	-111.6	-169.0
2000	-178.8	-116.7	-96.8	-96.8	-165.7
2500	-173.4	-103.1	-81.1	-82.0	-162.3
3000	-168.1	-89.4	-65.3	-67.2	-159.0
3500	-162.7	-75.7	-49.5	-52.4	-155.7
4000	-157.3	-62.1	-33.7	-37.6	-152.3
4500	-152.0	-48.4	-17.9	-22.7	-149.0
5000	-146.6	-34.7	-2.2	-7.9	-145.7
5500	-141.2	-21.1	13.6	6.9	-142.3
6000	-135.8	-7.4	29.4	21.7	-139.0
6500	-130.5	6.3	45.2	36.5	-135.7

[a] Calculated for a birch feedstock capacity level of 150 kt y^{-1}. (Orange fill: negative NPVs; Blue fill: positive NPVs).

Overall, despite the conservative hypotheses that were made in terms of CAPEX, this TEA shows that the DAOF can be economically viable. In this respect, the loading of dithionite and the *n*-butanol/water ratio applied were highlighted to have a decisive influence on the process profitability; the DAOF configuration employing a dithionite loading of 16.7% and an equivolumetric mixture of *n*-butanol and water appeared to be the most promising. Notably, the economic potential of DAOF was shown to be ultimately strongly dependent on the selling price for phenolic monomers.

Future work should focus on reducing the OPEX further to improve the economic feasibility of DAOF. The recovery of dithionite derivatives downstream and the regeneration of the reducing agent could be explored. In addition, the replacement of *n*-butanol with less expensive alcohols (*e.g.* methanol, ethanol) could contribute to diminish the operating costs.

DAOF of different lignocellulosic feedstocks

In order to explore the process robustness with respect to the treatment of lignocellulose from different sources, two herbaceous biomasses – miscanthus grass (*Miscanthus x giganteus*) and wheat straw (*Triticum aestivum*) – as well as a softwood (Norway spruce, *Picea abies*), were subjected to DAOF according to the conditions reported in Table 1, entry 9. The outcomes of the fractionation were compared to those observed for the treatment of birch sawdust. All biomasses possessed a particle size ≤ 2 mm.[49] Their composition is reported in Table S1.

Table S19 shows that larger yields of pulp were obtained for the treatment of miscanthus and spruce wood, in view of the higher cellulose content of these feedstocks. Birch wood led to the highest yield of OM in the organic fraction, likely due to a more facile lignin solvolysis for the case of hardwoods compared to softwoods and herbaceous biomass.[23] The largest yield of OM in the aqueous fraction was obtained for the processing of wheat straw, probably determined by the high content of water-soluble extractives in this biomass. Overall, a mass balance comprised between 78% (for birch wood) and 85% (for spruce wood) was obtained, highlighting that a partial conversion of biomass to volatiles occurred for all scenarios.

Table 4 Biomass derivatives obtained for the DAOF of different biomasses.

			Biomass[a]			
			Birch	Miscanthus	Wheat straw	Spruce
Solid fraction	Recovery (wt%)	C5	20 ± 2	24 ± 3	25 ± 2	30 ± 3
		C6	92 ± 2	96 ± 2	95 ± 3	94 ± 2
		Lignin[b]	27 ± 3	29 ± 3	36 ± 4	44 ± 2
	Conversion (%)	Glucan[c]	91 ± 5	92 ± 5	87 ± 7	38 ± 7
		Xylan[c]	94 ± 4	95 ± 4	89 ± 10	46 ± 2
	CI[d] (%)		57 ± 1	70 ± 3	70 ± 2	69 ± 4
Organic fraction	Yield (wt%)	Lignin oil[e]	93 ± 6	86 ± 1	94 ± 6	65 ± 2
		Monophenolics[e]	19.4 ± 1.8	13.1 ± 2.2	11.6 ± 1.6	7.3 ± 0.3
Aqueous fraction	Yield (wt%)	C5, C6 derivatives[f]	4.0 ± 0.4	3.1 ± 0.1	4.1 ± 0.5	3.6 ± 0.1

[a] Fractionation experiments were carried out treating 3 g o biomass (particle size < 2 mm) in 120 mL of a 50% v/v mixture of *n*-butanol and water, at 200 °C, under 30 bar of N_2 (introduced at ambient temperature), in the presence of $Na_2S_2O_4$ (16.7% w/w), for a duration of 3 hours. The reactions were carried out in duplicates.
[b] Acid-insoluble lignin
[c] The conversions of glucan and xylan for raw birch sawdust were 8% and 10%, respectively. For raw miscanthus they were 6% and 5%, respectively. For raw wheat straw they were 21% and 16%, respectively. For raw spruce sawdust they were 9% and 3%, respectively.
[d] The CI of raw birch sawdust was 49%. The CI of raw miscanthus was 64%. The CI of raw wheat straw was 63%. The CI of raw spruce sawdust was 62%.
[e] Expressed with respect to the weight of acid-insoluble lignin contained in the initial biomass.
[f] Non-condensed carbohydrate derivatives, expressed with respect to the total weight of polysaccharides contained in the initial biomass.

The properties of the different product streams obtained after DAOF of each feedstock are summarized in Table 4. Large recoveries of C6 polysaccharides in the pulp (≥90%) were determined for all scenarios, indicating excellent cellulose preservation. At the same time, hemicellulose was extensively solubilized, with a removal greater than 70%. A relatively low delignification was achieved for the treatment of spruce wood. A similar outcome was reported also for the organosolv and the RCF treatment of softwoods,[62,69] and the minor delignification was associated with the chemical structure of lignin that features a lower content of cleavable β-O-4 linkages, and a greater content of guaiacyl-units, possessing a higher tendency to undergo condensation reactions.[2,23,69] Another explanation for this behavior could be found in the generally less porous morphology of softwood biomass compared to hardwood and herbaceous feedstocks,[30,88] which may determine a higher mass transfer resistance for the solvolytic extraction

of lignin.[49] These findings were supported by further FTIR analyses of the solid fractions (Figure S16), which exhibited more apparent bands at 1160 cm^{-1} and the disappearance of the band at 1740 cm^{-1} for all biomasses, corresponding to a larger cellulose content and to the partial removal of hemicellulose and lignin, respectively. In addition, the bands at 1235 cm^{-1} and 1510 cm^{-1} (associated to hemicellulose and lignin) were found to vanish after treatment, and the band at 1595 cm^{-1} (associated to lignin) decreased for all feedstocks except spruce wood, confirming the less effective removal of lignin for softwood biomass. In line with these observations, the enzymatic convertibility of the isolated polysaccharides was considerably smaller for spruce wood compared to the other feedstocks, whose treatment led to highly digestible pulps (with convertibility ≥90%). On the other hand, the partial removal of amorphous components during DAOF resulted in a slight increase of the CI of the solid fractions for all biomass types (Table 4, Figure S17).

In agreement with the lower delignification observed for spruce wood, the yield of lignin oil isolated from the organic phase was modest for the treatment of this biomass. The GPC profiles of the lignin oils obtained from the treatment of the various feedstocks were different from one another (Figure 7a). A peak for monophenolics was observed in all cases, which became larger in the order: spruce wood < wheat straw < miscanthus < birch wood. A higher abundance of high M_W fragments was found for the treatment of wheat straw, as indicated by the more prominent peak at 350 g mol^{-1} and by the presence of an additional peak at 520 g mol^{-1}, as well as by the thick tail extending to higher molecular weights. These results suggest that a more effective depolymerization of lignin could be achieved when DAOF was applied to birch sawdust. Further inspection of the lignin oils via GC analysis corroborated the previous observations, with the greatest yield of monomers obtained for birch wood (19.4%), followed by miscanthus (13.1%), wheat straw (11.6%) and spruce wood (7.3%) (Figure 7b, Table 4). Remarkably, Figure 7b and

Table S20 show that, despite some variability in the yields of species with side chains containing carbonyl groups, a relatively high yield of monophenolics with 4-propenyl side chains was attained for all types of biomass employed, confirming that DAOF selectively promoted the reductive depolymerization of lignin from the various feedstocks.

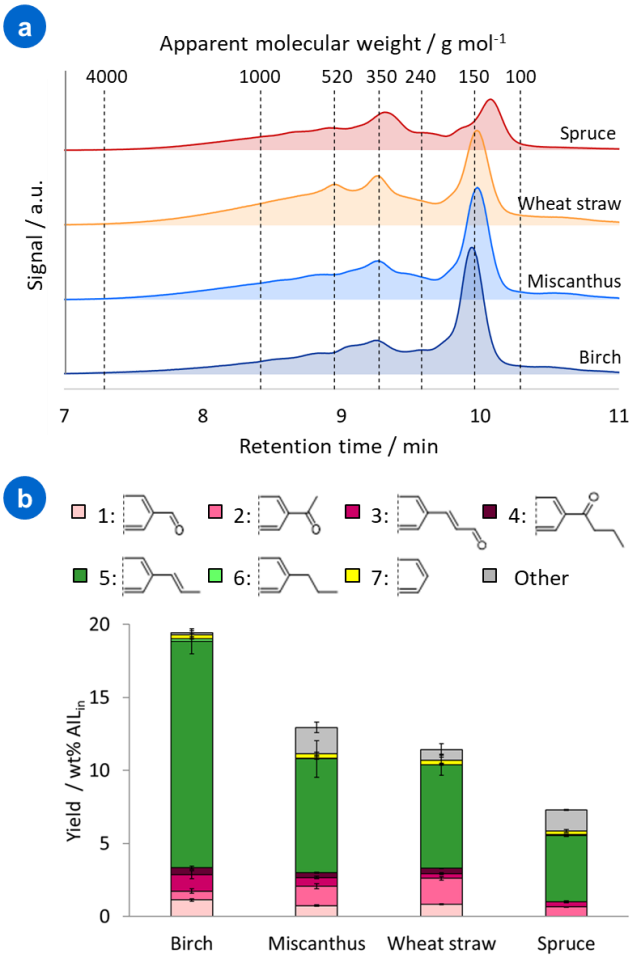

Figure 7 Comparison of the GPC chromatograms (a), and of the distribution of monophenolics as determined by GC (b) measured for the lignin oils isolated from the organic fractions obtained after treating different biomasses in 120 mL of a 50% v/v mixture of *n*-butanol and water, at 200 °C, under 30 bar of N_2 (introduced at ambient temperature), in the presence of $Na_2S_2O_4$ (16.7% $w/w_{biomass}$), for a duration of 3 hours. The area underneath each chromatogram was normalized with respect to the yield of lignin oil obtained for the corresponding experiment. The monomer yield was calculated with respect to the acid insoluble lignin (AIL) content in the initial biomass.

A generally low yield of non-condensed carbohydrate derivatives was observed for the treatment of the different biomasses (Figure S18), with a marginal release of xylose and the formation of low amounts of 1,2 propanediol and formic acid, confirming that the intermediates generated upon (hemi)cellulose decomposition are not promptly stabilized against recondensation during DAOF, regardless of the biomass source.

Overall, while all the explored lignocellulosic feedstocks were found to be suitable for DAOF, hardwood and herbaceous biomass appeared to be particularly prone to be valorized with this approach.

CONCLUSIONS

In this contribution, a dithionite-assisted organosolv fractionation in *n*-butanol and water is discussed, for the one-pot production of cellulosic pulp and mono-/oligo-aromatics from lignocellulose. With the goal of highlighting potentially profitable process configurations, the effect of process conditions, including the operating temperature and pressure, the loading of dithionite and that of biomass, the residence time, and the *n*-butanol/water ratio was investigated with respect to the properties of the isolated solid and liquid (organic and aqueous) fractions. Except for the exogenous N_2 pressure, all process variables were found to exert a remarkable influence on the yield and processability of the pulp, as well as on the yield of lignin oil and monophenolics. More specifically, the DAOF of birch wood performed at 200 °C for a duration of 3 to 6 hours in a mixture of *n*-butanol and water resulted in the extensive removal of hemicellulose (up to ~90%) and lignin (up to ~70%) from the biomass, as well as in the near complete preservation of highly digestible cellulose. In parallel, a lignin oil was isolated from the organic fraction with remarkable yields (> 84%, based on acid insoluble lignin), comprising

phenolic monomers, dimers and oligomers. Importantly, the loading of dithionite was found to have a major impact on lignin depolymerization and on the yield of monophenolics, which reached a maximum of ~20% (with a selectivity of 80% for 4-propenyl-substituted monoaromatics) for a loading of 16.7% w/$w_{biomass}$. On the other hand, the production of non-condensed carbohydrate derivatives in the aqueous fraction was found to be marginal for all the explored process configurations.

A techno-economic assessment of DAOF highlighted that, apart for the cost of the raw biomass itself, the cost of sodium dithionite and *n*-butanol represent the largest contribution to operational costs. The economic potential of DAOF was recognized to be strongly dependent on the market price of phenolic monomers and sensitivity analyses illustrated that a process configuration relying on a dithionite loading of 16.7% and on the use of an equivolumetric mixture of *n*-butanol and water would be the most profitable.

Moreover, the treatment of lignocellulosic biomass from various sources revealed that DAOF is a robust method, particularly suitable for processing hardwoods and herbaceous feedstocks, which resulted in high yields of digestible cellulosic pulp (with cellulose recoveries > 90%) and depolymerized lignin oil (~90%).

While alternative process configurations relying on less costly solvents (*e.g.* methanol, ethanol) and targeting the recovery and recycle of dithionite derivatives downstream should be envisaged, this study shows that DAOF is a promising and relatively facile method for integrating lignin valorization within biomass pretreatment, ultimately offering an innovative approach for the sustainable production of low-molecular weight aromatics from lignocellulose, in addition to a high-quality pulp.

ASSOCIATED CONTENT

Supporting information

The Supporting information is available free of charge. A complete description of the materials used in this work, of the experimental procedures adopted for carrying out fractionation experiments and for the analysis of the obtained product streams is given. Details of the calculations are provided. The supporting figures include the pictures of the experimental setup and of the fractionation products, ATR-FTIR spectra, XRD profiles, and SEM images of isolated pulps, ^{1}H-^{13}C HSQC NMR spectra of lignin oils, GPC profiles for dichloromethane and cyclohexane extracts, the pH of the aqueous fractions and the yields of non-condensed carbohydrate derivatives for the explored process configurations. The supporting tables provide details about the compositional analysis of the biomass feedstocks, OM contents of the isolated product streams, ATR-FTIR bands assignments, M_W of lignin oils, yields of phenolic monomers, ^{1}H-^{13}C HSQC NMR cross signals assignments and quantification, and the estimated CAPEX, OPEX, and revenues for different DAOF configurations.

AUTHOR INFORMATION

Corresponding Authors

* damien.debecker@uclouvain.be

* iwona.cybulska@uclouvain.be

Notes

The authors declare no competing financial interest.

ACKNOWLEDGMENT

This work was funded by an FSR grant (Fonds spéciaux de recherche) from UCLouvain. D. P. D. thanks the Francqui Foundation for his Francqui Research Professor Chair. K. V. A. acknowledges funding through FWO-SBO project BioWood and Catalisti-SBO project NIBCON. M. T. has received funding from the Research Foundation Flanders (FWO)-SBO BIOWOOD project. P.N. has received funding from the Energy Transition Fund ADV_BIO project, funded by the Belgian Federal Government's Department of Economy, General Direction of Energy. M. Leclercq and T. Nicolay are acknowledged for their help with assembling the experimental setup and with the development of GC-MS/FID methods. E. Devos is acknowledged for performing ICP-AES analyses.

REFERENCES

(1) Chandel, A. K.; Garlapati, V. K.; Singh, A. K.; Antunes, F. A. F.; da Silva, S. S. The Path Forward for Lignocellulose Biorefineries: Bottlenecks, Solutions, and Perspective on Commercialization. *Bioresource Technology* **2018**, *264*, 370–381. https://doi.org/10.1016/j.biortech.2018.06.004.

(2) Galkin, M. V.; Samec, J. S. M. Lignin Valorization through Catalytic Lignocellulose Fractionation: A Fundamental Platform for the Future Biorefinery. *ChemSusChem* **2016**, *9* (13), 1544–1558. https://doi.org/10.1002/cssc.201600237.

(3) Zakzeski, J.; Bruijnincx, P. C. A.; Jongerius, A. L.; Weckhuysen, B. M. The Catalytic Valorization of Lignin for the Production of Renewable Chemicals. *Chem. Rev.* **2010**, *110* (6), 3552–3599. https://doi.org/10.1021/cr900354u.

(4) Ragauskas, A. J.; Beckham, G. T.; Biddy, M. J.; Chandra, R.; Chen, F.; Davis, M. F.; Davison, B. H.; Dixon, R. A.; Gilna, P.; Keller, M.; Langan, P.; Naskar, A. K.; Saddler, J. N.; Tschaplinski, T. J.; Tuskan, G. A.; Wyman, C. E. Lignin Valorization: Improving Lignin Processing in the Biorefinery. *Science* **2014**, *344* (6185), 1246843–1246843. https://doi.org/10.1126/science.1246843.

(5) Arevalo-Gallegos, A.; Ahmad, Z.; Asgher, M.; Parra-Saldivar, R.; Iqbal, H. M. N. Lignocellulose: A Sustainable Material to Produce Value-Added Products with a Zero Waste Approach—A Review. *International Journal of Biological Macromolecules* **2017**, *99*, 308–318. https://doi.org/10.1016/j.ijbiomac.2017.02.097.

(6) Isikgor, F. H.; Becer, C. R. Lignocellulosic Biomass: A Sustainable Platform for the Production of Bio-Based Chemicals and Polymers. *Polym. Chem.* **2015**, *6* (25), 4497–4559. https://doi.org/10.1039/C5PY00263J.

(7) de Jong, E.; Gosselink, R. J. A. Lignocellulose-Based Chemical Products. In *Bioenergy Research: Advances and Applications*; Elsevier, 2014; pp 277–313. https://doi.org/10.1016/B978-0-444-59561-4.00017-6.

(8) Galbe, M.; Wallberg, O. Pretreatment for Biorefineries: A Review of Common Methods for Efficient Utilisation of Lignocellulosic Materials. *Biotechnol Biofuels* **2019**, *12* (1), 294. https://doi.org/10.1186/s13068-019-1634-1.
(9) Baruah, J.; Nath, B. K.; Sharma, R.; Kumar, S.; Deka, R. C.; Baruah, D. C.; Kalita, E. Recent Trends in the Pretreatment of Lignocellulosic Biomass for Value-Added Products. *Front. Energy Res.* **2018**, *6*, 141. https://doi.org/10.3389/fenrg.2018.00141.
(10) Ricardo Soccol, C.; Faraco, V.; Karp, S.; Vandenberghe, L. P. S.; Thomaz-Soccol, V.; Woiciechowski, A.; Pandey, A. Lignocellulosic Bioethanol. In *Biofuels*; Elsevier, 2011; pp 101–122. https://doi.org/10.1016/B978-0-12-385099-7.00005-X.
(11) Kang, S.; Fu, J.; Zhang, G. From Lignocellulosic Biomass to Levulinic Acid: A Review on Acid-Catalyzed Hydrolysis. *Renewable and Sustainable Energy Reviews* **2018**, *94*, 340–362. https://doi.org/10.1016/j.rser.2018.06.016.
(12) Xu, C.; Paone, E.; Rodríguez-Padrón, D.; Luque, R.; Mauriello, F. Recent Catalytic Routes for the Preparation and the Upgrading of Biomass Derived Furfural and 5-Hydroxymethylfurfural. *Chem. Soc. Rev.* **2020**, *49* (13), 4273–4306. https://doi.org/10.1039/D0CS00041H.
(13) Liao, Y.; Koelewijn, S.-F.; Van den Bossche, G.; Van Aelst, J.; Van den Bosch, S.; Renders, T.; Navare, K.; Nicolaï, T.; Van Aelst, K.; Maesen, M.; Matsushima, H.; Thevelein, J. M.; Van Acker, K.; Lagrain, B.; Verboekend, D.; Sels, B. F. A Sustainable Wood Biorefinery for Low–Carbon Footprint Chemicals Production. *Science* **2020**, *367* (6484), 1385–1390. https://doi.org/10.1126/science.aau1567.
(14) Schutyser, W.; Van den Bosch, S.; Dijkmans, J.; Turner, S.; Meledina, M.; Van Tendeloo, G.; Debecker, D. P.; Sels, B. F. Selective Nickel-Catalyzed Conversion of Model and Lignin-Derived Phenolic Compounds to Cyclohexanone-Based Polymer Building Blocks. *ChemSusChem* **2015**, *8* (10), 1805–1818. https://doi.org/10.1002/cssc.201403375.
(15) Deneyer, A.; Peeters, E.; Renders, T.; Van den Bosch, S.; Van Oeckel, N.; Ennaert, T.; Szarvas, T.; Korányi, T. I.; Dusselier, M.; Sels, B. F. Direct Upstream Integration of Biogasoline Production into Current Light Straight Run Naphtha Petrorefinery Processes. *Nat Energy* **2018**, *3* (11), 969–977. https://doi.org/10.1038/s41560-018-0245-6.
(16) Mayer-Laigle, C.; Blanc, N.; Rajaonarivony, R.; Rouau, X. Comminution of Dry Lignocellulosic Biomass, a Review: Part I. From Fundamental Mechanisms to Milling Behaviour. *Bioengineering* **2018**, *5* (2), 41. https://doi.org/10.3390/bioengineering5020041.
(17) Mayer-Laigle, C.; Rajaonarivony, R.; Blanc, N.; Rouau, X. Comminution of Dry Lignocellulosic Biomass: Part II. Technologies, Improvement of Milling Performances, and Security Issues. *Bioengineering* **2018**, *5* (3), 50. https://doi.org/10.3390/bioengineering5030050.
(18) Bussemaker, M. J.; Zhang, D. Effect of Ultrasound on Lignocellulosic Biomass as a Pretreatment for Biorefinery and Biofuel Applications. *Ind. Eng. Chem. Res.* **2013**, *52* (10), 3563–3580. https://doi.org/10.1021/ie3022785.
(19) Kim, J. S.; Lee, Y. Y.; Kim, T. H. A Review on Alkaline Pretreatment Technology for Bioconversion of Lignocellulosic Biomass. *Bioresource Technology* **2016**, *199*, 42–48. https://doi.org/10.1016/j.biortech.2015.08.085.
(20) Lachenal, D. Kraft Pulping. In *Lignocellulosic Fibers and Wood Handbook*; Belgacem, N., Pizzi, A., Eds.; John Wiley & Sons, Inc.: Hoboken, NJ, USA, 2016; pp 207–223. https://doi.org/10.1002/9781118773727.ch7.

(21) Zhang, J.; Bao, J. Lignocellulose Pretreatment Using Acid as Catalyst. In *Handbook of Biorefinery Research and Technology*; Park, J. M., Ed.; Springer Netherlands: Dordrecht, 2018; pp 1–14. https://doi.org/10.1007/978-94-007-6724-9_3-1.
(22) Evtuguin, D. V. Sulphite Pulping. In *Lignocellulosic Fibers and Wood Handbook*; Belgacem, N., Pizzi, A., Eds.; John Wiley & Sons, Inc.: Hoboken, NJ, USA, 2016; pp 225–244. https://doi.org/10.1002/9781118773727.ch8.
(23) Wei Kit Chin, D.; Lim, S.; Pang, Y. L.; Lam, M. K. Fundamental Review of Organosolv Pretreatment and Its Challenges in Emerging Consolidated Bioprocessing. *Biofuels, Bioprod. Bioref.* **2020**, *14* (4), 808–829. https://doi.org/10.1002/bbb.2096.
(24) Thoresen, P. P.; Matsakas, L.; Rova, U.; Christakopoulos, P. Recent Advances in Organosolv Fractionation: Towards Biomass Fractionation Technology of the Future. *Bioresource Technology* **2020**, *306*, 123189. https://doi.org/10.1016/j.biortech.2020.123189.
(25) Brandt, A.; Gräsvik, J.; Hallett, J. P.; Welton, T. Deconstruction of Lignocellulosic Biomass with Ionic Liquids. *Green Chem.* **2013**, *15* (3), 550. https://doi.org/10.1039/c2gc36364j.
(26) Duque, A.; Manzanares, P.; Ballesteros, I.; Ballesteros, M. Steam Explosion as Lignocellulosic Biomass Pretreatment. In *Biomass Fractionation Technologies for a Lignocellulosic Feedstock Based Biorefinery*; Elsevier, 2016; pp 349–368. https://doi.org/10.1016/B978-0-12-802323-5.00015-3.
(27) Balan, V.; Bals, B.; Chundawat, S. P. S.; Marshall, D.; Dale, B. E. Lignocellulosic Biomass Pretreatment Using AFEX. In *Biofuels*; Mielenz, J. R., Ed.; Methods in Molecular Biology; Humana Press: Totowa, NJ, 2009; Vol. 581, pp 61–77. https://doi.org/10.1007/978-1-60761-214-8_5.
(28) Key, R. E.; Bozell, J. J. Progress toward Lignin Valorization via Selective Catalytic Technologies and the Tailoring of Biosynthetic Pathways. *ACS Sustainable Chem. Eng.* **2016**, *4* (10), 5123–5135. https://doi.org/10.1021/acssuschemeng.6b01319.
(29) Rinaldi, R.; Jastrzebski, R.; Clough, M. T.; Ralph, J.; Kennema, M.; Bruijnincx, P. C. A.; Weckhuysen, B. M. Paving the Way for Lignin Valorisation: Recent Advances in Bioengineering, Biorefining and Catalysis. *Angew. Chem. Int. Ed.* **2016**, *55* (29), 8164–8215. https://doi.org/10.1002/anie.201510351.
(30) Schutyser, W.; Renders, T.; Van den Bosch, S.; Koelewijn, S.-F.; Beckham, G. T.; Sels, B. F. Chemicals from Lignin: An Interplay of Lignocellulose Fractionation, Depolymerisation, and Upgrading. *Chem. Soc. Rev.* **2018**, *47* (3), 852–908. https://doi.org/10.1039/C7CS00566K.
(31) Van den Bosch, S.; Koelewijn, S.-F.; Renders, T.; Van den Bossche, G.; Vangeel, T.; Schutyser, W.; Sels, B. F. Catalytic Strategies Towards Lignin-Derived Chemicals. *Top Curr Chem (Z)* **2018**, *376* (5), 36. https://doi.org/10.1007/s41061-018-0214-3.
(32) Sun, Z.; Fridrich, B.; de Santi, A.; Elangovan, S.; Barta, K. Bright Side of Lignin Depolymerization: Toward New Platform Chemicals. *Chem. Rev.* **2018**, *118* (2), 614–678. https://doi.org/10.1021/acs.chemrev.7b00588.
(33) Cao, L.; Yu, I. K. M.; Liu, Y.; Ruan, X.; Tsang, D. C. W.; Hunt, A. J.; Ok, Y. S.; Song, H.; Zhang, S. Lignin Valorization for the Production of Renewable Chemicals: State-of-the-Art Review and Future Prospects. *Bioresource Technology* **2018**, *269*, 465–475. https://doi.org/10.1016/j.biortech.2018.08.065.
(34) Kawamoto, H. Molecular Mechanisms in the Thermochemical Conversion of Lignins into Bio-Oil/Chemicals and Biofuels. In *Production of Biofuels and Chemicals from Lignin*;

Fang, Z., Smith, R. L., Eds.; Biofuels and Biorefineries; Springer Singapore: Singapore, 2016; pp 321–353. https://doi.org/10.1007/978-981-10-1965-4_11.
(35) Liakakou, E. T.; Vreugdenhil, B. J.; Cerone, N.; Zimbardi, F.; Pinto, F.; André, R.; Marques, P.; Mata, R.; Girio, F. Gasification of Lignin-Rich Residues for the Production of Biofuels via Syngas Fermentation: Comparison of Gasification Technologies. *Fuel* **2019**, *251*, 580–592. https://doi.org/10.1016/j.fuel.2019.04.081.
(36) Abu-Omar, M. M.; Barta, K.; Beckham, G. T.; Luterbacher, J. S.; Ralph, J.; Rinaldi, R.; Román-Leshkov, Y.; Samec, J. S. M.; Sels, B. F.; Wang, F. Guidelines for Performing Lignin-First Biorefining. *Energy Environ. Sci.* **2021**, 262–292. https://doi.org/10.1039/D0EE02870C.
(37) Korányi, T. I.; Fridrich, B.; Pineda, A.; Barta, K. Development of 'Lignin-First' Approaches for the Valorization of Lignocellulosic Biomass. *Molecules* **2020**, *25* (12), 2815. https://doi.org/10.3390/molecules25122815.
(38) Questell-Santiago, Y. M.; Galkin, M. V.; Barta, K.; Luterbacher, J. S. Stabilization Strategies in Biomass Depolymerization Using Chemical Functionalization. *Nat Rev Chem* **2020**, *4* (6), 311–330. https://doi.org/10.1038/s41570-020-0187-y.
(39) Luo, X.; Li, Y.; Gupta, N. K.; Sels, B.; Ralph, J.; Shuai, L. Protection Strategies Enable Selective Conversion of Biomass. *Angew. Chem.* **2020**, *132* (29), 11800–11812. https://doi.org/10.1002/ange.201914703.
(40) Renders, T.; Van den Bosch, S.; Koelewijn, S.-F.; Schutyser, W.; Sels, B. F. Lignin-First Biomass Fractionation: The Advent of Active Stabilisation Strategies. *Energy Environ. Sci.* **2017**, *10* (7), 1551–1557. https://doi.org/10.1039/C7EE01298E.
(41) Renders, T.; Van den Bossche, G.; Vangeel, T.; Van Aelst, K.; Sels, B. Reductive Catalytic Fractionation: State of the Art of the Lignin-First Biorefinery. *Current Opinion in Biotechnology* **2019**, *56*, 193–201. https://doi.org/10.1016/j.copbio.2018.12.005.
(42) Cooreman, E.; Vangeel, T.; Van Aelst, K.; Van Aelst, J.; Lauwaert, J.; Thybaut, J. W.; Van den Bosch, S.; Sels, B. F. Perspective on Overcoming Scale-Up Hurdles for the Reductive Catalytic Fractionation of Lignocellulose Biomass. *Ind. Eng. Chem. Res.* **2020**, *59* (39), 17035–17045. https://doi.org/10.1021/acs.iecr.0c02294.
(43) Van den Bosch, S.; Renders, T.; Kennis, S.; Koelewijn, S.-F.; Van den Bossche, G.; Vangeel, T.; Deneyer, A.; Depuydt, D.; Courtin, C. M.; Thevelein, J. M.; Schutyser, W.; Sels, B. F. Integrating Lignin Valorization and Bio-Ethanol Production: On the Role of Ni-Al $_2$ O $_3$ Catalyst Pellets during Lignin-First Fractionation. *Green Chem.* **2017**, *19* (14), 3313–3326. https://doi.org/10.1039/C7GC01324H.
(44) Klinger, G. E.; Zhou, Y.; Foote, J. A.; Wester, A. M.; Cui, Y.; Alherech, M.; Stahl, S. S.; Jackson, J. E.; Hegg, E. L. Nucleophilic Thiols Reductively Cleave Ether Linkages in Lignin Model Polymers and Lignin. *ChemSusChem* **2020**, *13* (17), 4394–4399. https://doi.org/10.1002/cssc.202001238.
(45) Klinger, G. E.; Zhou, Y.; Hao, P.; Robbins, J.; Aquilina, J. M.; Jackson, J. E.; Hegg, E. L. Biomimetic Reductive Cleavage of Keto Aryl Ether Bonds by Small-Molecule Thiols. *ChemSusChem* **2019**, *12* (21), 4775–4779. https://doi.org/10.1002/cssc.201901742.
(46) Fang, Z.; Flynn, M. G.; Jackson, J. E.; Hegg, E. L. Thio-Assisted Reductive Electrolytic Cleavage of Lignin β-O-4 Models and Authentic Lignin. *Green Chem.* **2021**, *23* (1), 412–421. https://doi.org/10.1039/D0GC03597A.
(47) Brienza, F.; Van Aelst, K.; Thielemans, K.; Sels, B. F.; Debecker, D. P.; Cybulska, I. Enhancing Lignin Depolymerization *via* a Dithionite-Assisted Organosolv Fractionation of

Birch Sawdust. *Green Chem.* **2021**, *23* (9), 3268–3276. https://doi.org/10.1039/D1GC00503K.
(48) Cybulska, I.; Brienza, F.; Debecker, D. P. Process for Producing Lignin Components from Lignocellulosic Biomass. WO2021058483, April 1, 2021.
(49) Thornburg, N. E.; Pecha, M. B.; Brandner, D. G.; Reed, M. L.; Vermaas, J. V.; Michener, W. E.; Katahira, R.; Vinzant, T. B.; Foust, T. D.; Donohoe, B. S.; Román-Leshkov, Y.; Ciesielski, P. N.; Beckham, G. T. Mesoscale Reaction–Diffusion Phenomena Governing Lignin-First Biomass Fractionation. *ChemSusChem* **2020**, *13* (17), 4495–4509. https://doi.org/10.1002/cssc.202000558.
(50) Cybulska, I.; Chaturvedi, T.; Thomsen, M. H. Lignocellulosic Thermochemical Pretreatment Processes. In *Biorefinery*; Bastidas-Oyanedel, J.-R., Schmidt, J. E., Eds.; Springer International Publishing: Cham, 2019; pp 153–165. https://doi.org/10.1007/978-3-030-10961-5_6.
(51) Kawamata, Y.; Yoshikawa, T.; Nakasaka, Y.; Koyama, Y.; Fumoto, E.; Sato, S.; Tago, T.; Masuda, T. Organosolv Treatment Using 1-Butanol and Degradation of Extracted Lignin Fractions into Phenolic Compounds over Iron Oxide Catalyst. *J. Jpn. Petrol. Inst.* **2019**, *62* (1), 37–44. https://doi.org/10.1627/jpi.62.37.
(52) Paksung, N.; Matsumura, Y. Decomposition of Xylose in Sub- and Supercritical Water. *Ind. Eng. Chem. Res.* **2015**, *54* (31), 7604–7613. https://doi.org/10.1021/acs.iecr.5b01623.
(53) Jing, Q.; Lü, X. Kinetics of Non-Catalyzed Decomposition of D-Xylose in High Temperature Liquid Water. *Chinese Journal of Chemical Engineering* **2007**, *15* (5), 666–669. https://doi.org/10.1016/S1004-9541(07)60143-8.
(54) Gosselink, R. J. A.; van Dam, J. E. G.; Zomers, F. H. A. Combined HPLC Analysis of Organic Acids and Furans Formed During Organosolv Pulping of Fiber Hemp. *Journal of Wood Chemistry and Technology* **1995**, *15* (1), 1–25. https://doi.org/10.1080/02773819508009497.
(55) Schutyser, W.; Van den Bosch, S.; Renders, T.; De Boe, T.; Koelewijn, S.-F.; Dewaele, A.; Ennaert, T.; Verkinderen, O.; Goderis, B.; Courtin, C. M.; Sels, B. F. Influence of Bio-Based Solvents on the Catalytic Reductive Fractionation of Birch Wood. *Green Chem.* **2015**, *17* (11), 5035–5045. https://doi.org/10.1039/C5GC01442E.
(56) Shuai, L.; Luterbacher, J. Organic Solvent Effects in Biomass Conversion Reactions. *ChemSusChem* **2016**, *9* (2), 133–155. https://doi.org/10.1002/cssc.201501148.
(57) Balogh, D. T.; Curvelo, A. A. S.; De Groote, R. A. M. C. Solvent Effects on Organosolv Lignin from *Pinus Caribaea Hondurensis*. *Holzforschung* **1992**, *46* (4), 343–348. https://doi.org/10.1515/hfsg.1992.46.4.343.
(58) Crocker, D.; Templeton, D.; Sluiter, J.; Scarlata, C.; Ruiz, R.; Hames, B.; Sluiter, A. *Determination of Structural Carbohydrates and Lignin in Biomass*; National Renewable Energy Laboratory, Golden, CO, USA, 2012.
(59) Segal, L.; Creely, J. J.; Martin, A. E.; Conrad, C. M. An Empirical Method for Estimating the Degree of Crystallinity of Native Cellulose Using the X-Ray Diffractometer. *Textile Research Journal* **1959**, *29* (10), 786–794. https://doi.org/10.1177/004051755902901003.
(60) Selig, M.; Weiss, N.; Ji, Y. *Enzymatic Saccharification of Lignocellulosic Biomass*; National Renewable Energy Laboratory, Golden, CO, USA, 2008.
(61) Hu, F.; Jung, S.; Ragauskas, A. Pseudo-Lignin Formation and Its Impact on Enzymatic Hydrolysis. *Bioresource Technology* **2012**, *117*, 7–12. https://doi.org/10.1016/j.biortech.2012.04.037.

(62) Schmetz, Q.; Teramura, H.; Morita, K.; Oshima, T.; Richel, A.; Ogino, C.; Kondo, A. Versatility of a Dilute Acid/Butanol Pretreatment Investigated on Various Lignocellulosic Biomasses to Produce Lignin, Monosaccharides and Cellulose in Distinct Phases. *ACS Sustainable Chem. Eng.* **2019**, *7* (13), 11069–11079. https://doi.org/10.1021/acssuschemeng.8b05841.
(63) Shinde, S. D.; Meng, X.; Kumar, R.; Ragauskas, A. J. Recent Advances in Understanding the Pseudo-Lignin Formation in a Lignocellulosic Biorefinery. *Green Chem.* **2018**, *20* (10), 2192–2205. https://doi.org/10.1039/C8GC00353J.
(64) Sun, Q.; Foston, M.; Meng, X.; Sawada, D.; Pingali, S. V.; O'Neill, H. M.; Li, H.; Wyman, C. E.; Langan, P.; Ragauskas, A. J.; Kumar, R. Effect of Lignin Content on Changes Occurring in Poplar Cellulose Ultrastructure during Dilute Acid Pretreatment. *Biotechnol Biofuels* **2014**, *7* (1), 150. https://doi.org/10.1186/s13068-014-0150-6.
(65) Tu, W.-C.; Weigand, L.; Hummel, M.; Sixta, H.; Brandt-Talbot, A.; Hallett, J. P. Characterisation of Cellulose Pulps Isolated from Miscanthus Using a Low-Cost Acidic Ionic Liquid. *Cellulose* **2020**, *27* (8), 4745–4761. https://doi.org/10.1007/s10570-020-03073-1.
(66) Liao, Y.; de Beeck, B. O.; Thielemans, K.; Ennaert, T.; Snelders, J.; Dusselier, M.; Courtin, C. M.; Sels, B. F. The Role of Pretreatment in the Catalytic Valorization of Cellulose. *Molecular Catalysis* **2020**, *487*, 110883. https://doi.org/10.1016/j.mcat.2020.110883.
(67) Garrote, G.; Domínguez, H.; Parajó, J. C. Study on the Deacetylation of Hemicelluloses during the Hydrothermal Processing of Eucalyptus Wood. *Holz als Roh- und Werkstoff* **2001**, *59* (1–2), 53–59. https://doi.org/10.1007/s001070050473.
(68) Agarwal, U. P.; Reiner, R. R.; Ralph, S. A. Estimation of Cellulose Crystallinity of Lignocelluloses Using Near-IR FT-Raman Spectroscopy and Comparison of the Raman and Segal-WAXS Methods. *J. Agric. Food Chem.* **2013**, *61* (1), 103–113. https://doi.org/10.1021/jf304465k.
(69) Van den Bosch, S.; Schutyser, W.; Vanholme, R.; Driessen, T.; Koelewijn, S.-F.; Renders, T.; De Meester, B.; Huijgen, W. J. J.; Dehaen, W.; Courtin, C. M.; Lagrain, B.; Boerjan, W.; Sels, B. F. Reductive Lignocellulose Fractionation into Soluble Lignin-Derived Phenolic Monomers and Dimers and Processable Carbohydrate Pulps. *Energy Environ. Sci.* **2015**, *8* (6), 1748–1763. https://doi.org/10.1039/C5EE00204D.
(70) Borand, M. N.; Karaosmanoğlu, F. Effects of Organosolv Pretreatment Conditions for Lignocellulosic Biomass in Biorefinery Applications: A Review. *Journal of Renewable and Sustainable Energy* **2018**, *10* (3), 033104. https://doi.org/10.1063/1.5025876.
(71) Rinaldi, R.; Woodward, R.; Ferrini, P.; Rivera, H. Lignin-First Biorefining of Lignocellulose: The Impact of Process Severity on the Uniformity of Lignin Oil Composition. *J. Braz. Chem. Soc.* **2018**. https://doi.org/10.21577/0103-5053.20180231.
(72) van Zandvoort, I.; Wang, Y.; Rasrendra, C. B.; van Eck, E. R. H.; Bruijnincx, P. C. A.; Heeres, H. J.; Weckhuysen, B. M. Formation, Molecular Structure, and Morphology of Humins in Biomass Conversion: Influence of Feedstock and Processing Conditions. *ChemSusChem* **2013**, *6* (9), 1745–1758. https://doi.org/10.1002/cssc.201300332.
(73) Cheng, Z.; Everhart, J. L.; Tsilomelekis, G.; Nikolakis, V.; Saha, B.; Vlachos, D. G. Structural Analysis of Humins Formed in the Brønsted Acid Catalyzed Dehydration of Fructose. *Green Chem.* **2018**, *20* (5), 997–1006. https://doi.org/10.1039/C7GC03054A.

(74) Lem, W. J.; Wayman, M. Decomposition of Aqueous Dithionite. Part I. Kinetics of Decomposition of Aqueous Sodium Dithionite. *Can. J. Chem.* **1970**, *48* (5), 776–781. https://doi.org/10.1139/v70-126.
(75) Wayman, M.; Lem, W. J. Decomposition of Aqueous Dithionite. Part II. A Reaction Mechanism for the Decomposition of Aqueous Sodium Dithionite. *Can. J. Chem.* **1970**, *48* (5), 782–787. https://doi.org/10.1139/v70-127.
(76) Rinker, R. G.; Lynn, S.; Mason, D. M.; Corcoran, W. H. Kinetics and Mechanism of Thermal Decomposition of Sodium Dithionite in Aqueous Solution. *Ind. Eng. Chem. Fund.* **1965**, *4* (3), 282–288. https://doi.org/10.1021/i160015a008.
(77) Burlamacchi, L.; Guarini, G.; Tiezzi, E. Mechanism of Decomposition of Sodium Dithionite in Aqueous Solution. *Trans. Faraday Soc.* **1969**, *65*, 496. https://doi.org/10.1039/tf9696500496.
(78) Ferrini, P.; Rinaldi, R. Catalytic Biorefining of Plant Biomass to Non-Pyrolytic Lignin Bio-Oil and Carbohydrates through Hydrogen Transfer Reactions. *Angew. Chem. Int. Ed.* **2014**, *53* (33), 8634–8639. https://doi.org/10.1002/anie.201403747.
(79) Van Aelst, K.; Van Sinay, E.; Vangeel, T.; Cooreman, E.; Van den Bossche, G.; Renders, T.; Van Aelst, J.; Van den Bosch, S.; Sels, B. F. Reductive Catalytic Fractionation of Pine Wood: Elucidating and Quantifying the Molecular Structures in the Lignin Oil. *Chem. Sci.* **2020**, *11* (42), 11498–11508. https://doi.org/10.1039/D0SC04182C.
(80) Liao, Y.; Koelewijn, S.-F.; Van den Bossche, G.; Van Aelst, J.; Van den Bosch, S.; Renders, T.; Navare, K.; Nicolaï, T.; Van Aelst, K.; Maesen, M.; Matsushima, H.; Thevelein, J. M.; Van Acker, K.; Lagrain, B.; Verboekend, D.; Sels, B. F. A Sustainable Wood Biorefinery for Low–Carbon Footprint Chemicals Production. *Science* **2020**, *367* (6484), 1385–1390. https://doi.org/10.1126/science.aau1567.
(81) Ebikade, O. E.; Samulewicz, N.; Xuan, S.; Sheehan, J. D.; Wu, C.; Vlachos, D. G. Reductive Catalytic Fractionation of Agricultural Residue and Energy Crop Lignin and Application of Lignin Oil in Antimicrobials. *Green Chem.* **2020**, *22* (21), 7435–7447. https://doi.org/10.1039/D0GC02781B.
(82) Renders, T.; Cooreman, E.; Van den Bosch, S.; Schutyser, W.; Koelewijn, S.-F.; Vangeel, T.; Deneyer, A.; Van den Bossche, G.; Courtin, C. M.; Sels, B. F. Catalytic Lignocellulose Biorefining in *n* -Butanol/Water: A One-Pot Approach toward Phenolics, Polyols, and Cellulose. *Green Chem.* **2018**, *20* (20), 4607–4619. https://doi.org/10.1039/C8GC01031E.
(83) Ferrini, P.; Rezende, C. A.; Rinaldi, R. Catalytic Upstream Biorefining through Hydrogen Transfer Reactions: Understanding the Process from the Pulp Perspective. *ChemSusChem* **2016**, *9* (22), 3171–3180. https://doi.org/10.1002/cssc.201601121.
(84) Chemical Pulping Processe: Sections 4.2.8–4.3.6.5. In *Handbook of Pulp*; Sixta, H., Ed.; Wiley-VCH Verlag GmbH: Weinheim, Germany, 2006; pp 366–509. https://doi.org/10.1002/9783527619887.ch4c.
(85) Sixta, H.; Potthast, A.; Krotschek, A. W. Chemical Pulping Processe: Sections 4.1–4.2.5. In *Handbook of Pulp*; Sixta, H., Ed.; Wiley-VCH Verlag GmbH: Weinheim, Germany, 2006; pp 109–229. https://doi.org/10.1002/9783527619887.ch4a.
(86) Tschulkow, M.; Compernolle, T.; Van den Bosch, S.; Van Aelst, J.; Storms, I.; Van Dael, M.; Van den Bossche, G.; Sels, B.; Van Passel, S. Integrated Techno-Economic Assessment of a Biorefinery Process: The High-End Valorization of the Lignocellulosic Fraction in Wood Streams. *Journal of Cleaner Production* **2020**, *266*, 122022. https://doi.org/10.1016/j.jclepro.2020.122022.

(87) Gillet, S.; Aguedo, M.; Petitjean, L.; Morais, A. R. C.; da Costa Lopes, A. M.; Łukasik, R. M.; Anastas, P. T. Lignin Transformations for High Value Applications: Towards Targeted Modifications Using Green Chemistry. *Green Chem.* **2017**, *19* (18), 4200–4233. https://doi.org/10.1039/C7GC01479A.
(88) Ansell, M. P. Wood Microstructure – A Cellular Composite. In *Wood Composites*; Elsevier, 2015; pp 3–26. https://doi.org/10.1016/B978-1-78242-454-3.00001-9.